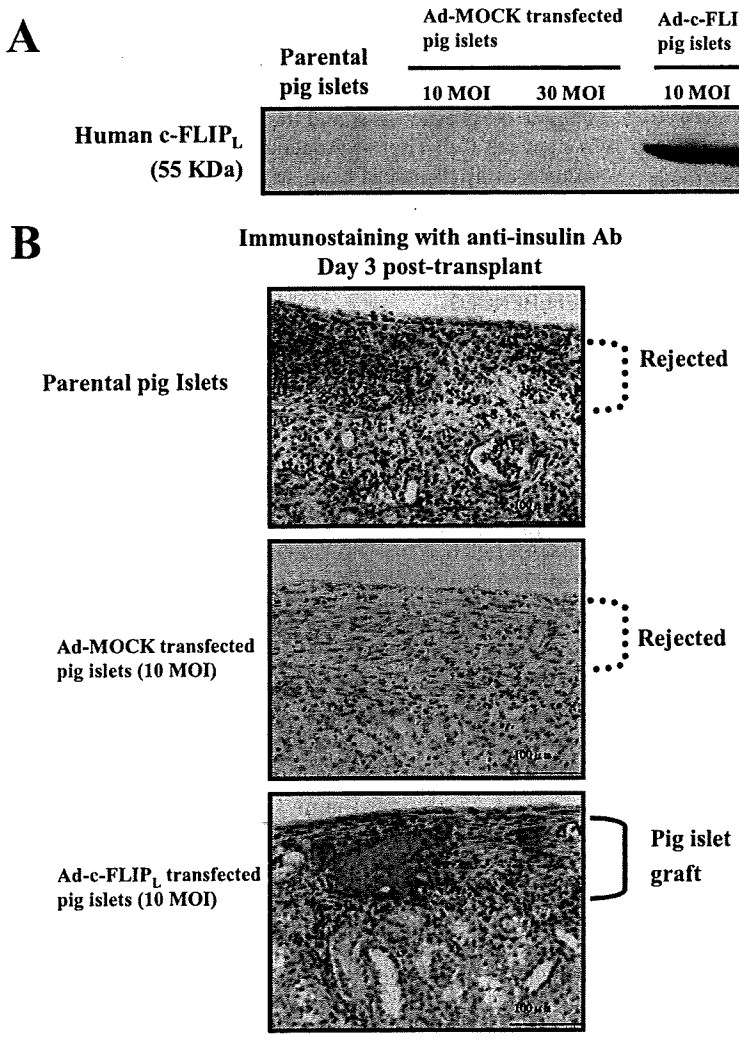

Fig 1. (A) The intracellular expression of c-FLIP$_L$ protein. Adenovirus-mediated gene expression of human c-FLIP$_L$ protein was assessed by Western blot analysis. **(B)** Immunohistological findings of rat kidney tissue of pig islets transplanted rats. Immunostaining with anti-pig insulin Ab for transplanted pig islet xenografts obtained at day 3 post-transplant. The black bars in each picture indicated 100 μm.

control adenovirus vector did not exhibit protein expression of c-FLIP$_L$ at adenovirus concentrations of 10 and 30 MOI. In contrast, transduction with adenovirus vector containing complementary DNA of c-FLIP$_L$ resulted in distinct expression of this molecule at 10 and 30 MOI. The expression level of c-FLIP$_L$ was similar compared with adenovirus transduction of 10 and 30 MOI (Fig 1A).

Adenovirus Expression of c-FLIP$_L$ Effectively Inhibits Cytotoxicity of Human CD8+ CTLs Against Pig Islet Cells

Human CD8+ CTLs generated by in vitro culture exhibited strong direct killing against parental and mock islets. Approximately, 60% lysis of both parental and mock islets was evident in these human CTLs at an effector-to-target ratio of 50:1 (Table 1). In contrast, the cytotoxicity was significantly reduced against pig islet cells transduced with the c-FLIP$_L$ adenovirus vector, that is, 52% inhibition at an effector-to-target ratio of 50:1 (Table 1).

Prolonged Xenograft Survival Was Elicited From c-FLIP$_L$-Transfected Pig Islet Cells

To determine whether adenovirus expression of c-FLIP$_L$ in pig islets can prolong xenograft survival, we transplanted pig islets under the kidney capsule in rats. The results of immunohistochemical analysis are shown in Fig 1B. At day 2 posttransplantation, parental, MOCK, and transfected pig islet xenografts survived under the kidney capsule (data not shown). At day 3 posttransplantation, parental and MOCK pig islet xenografts were completely rejected (Fig 1B). In contrast, pig islet xenografts expressing c-FLIP$_L$ survived intact as judged by insulin staining (Fig 1B). At day 5 posttransplantation, pig islet xenografts expressing c-FLIP$_L$ still exhibited insulin staining despite reduced graft size (data not shown). These findings demonstrate the beneficial effects of both in vitro and in vivo cytoprotection of pig islet xenografts expressing c-FLIP$_L$.

Table 1. ^{51}Cr Release in Pig Islets

Pig Islets	Adenovirus Concentration, MOI	Percent Cytotoxicity at ^{51}Cr Release Assay, Mean (SD)	
		E/T Ratio 50:1	E/T Ratio 25:1
Parental		59.3 (15.9)	47.6 (8.2)
Mock (control	10	64.0 (8.9)	48.7 (14.8)
adenovirus	30	59.0 (1.4)	43.3 (5.5)
transfected pig islets)			
c-FLIP$_L$ transfected	10	30.5 (3.5)*	24.3 (1.6)*
pig islets	30	23.6 (11.6)*	21.0 (11.0)*

Abbreviations: ^{51}Cr, chromium 51; E/T, effector-target; cFLIP$_L$, cellular FLICE-like inhibitory protein, long form; MOI, multiplicity of infection.

Amelioration of human CD8+ cytotoxic T lymphocyte–mediated cytotoxicity by transduced pig islets was assessed by ^{5}Cr release assay Control parental and mock pig islets were estimated at the E/T Ratio of either 25:1 or 50:1. Values are given as the mean (SD) from five independent experiments.

*Difference statistically significant ($P < .05$, c-FLIP$_L$-transfected pig islets vs parental and mock pig islets).

DISCUSSION

In the present study, we determined that the expression of human c-FLIP$_L$ can be induced in pig islet cells using adenovirus vectors. Pig islet xenografts expressing this molecule were markedly protected from direct human CD8+ CTL-mediated lysis. Furthermore, beneficial effects of in vivo prolongation of pig islet xenografts with adenoviral expression of c-FLIP$_L$ were demonstrated.

It is generally thought that the adenoviral vector is not able to penetrate more than a few cell layers. In a previous study, we demonstrated that the virus vector used was able to infect more than 80% of islet cells, as assessed using fluorescence-activated cell sorting, and that protein expression in big islets was restricted to the outer cell layers.[13,14] In addition, because the new DNA is not integrated into the genome of the infected cells, the gene expression is only transient. The strategy of adenovirus-mediated expression in pig islet cells may have only restricted application to clinical islet xenotransplantation. Another strategy would be to generate transgenic pigs expressing the c-FLIP$_L$ molecule in the islet cells. However, in the study in which islets isolated from transgenic pigs expressed high levels of human decay-accelerating factor on endothelial cells, no or only minimal levels of this factor were detected on the islet cells.[15] Therefore, these findings indicate that transgenic pigs, in which the gene constructs containing c-FLIP$_L$ may be regulated by, for example, the insulin promoter, will have to be created to provide sufficient cytoprotection against CD8+ CTL cytotoxicity in pig islet xenotransplantation.

In this pig islet transplant model, large infiltrations of both CD8+ T cells and macrophages were detected. A large number of macrophages infiltrating pig islet xenografts secret inflammatory cytokines including IL-1β, tumor necrosis factor–α, and interferon-γ, which may induce β-cell damage through activation of several intracellular stress-signaling pathways.[16] Our preliminary data suggest that pig islet cells expressing c-FLIP$_L$ induce resistance against cytokine exposure containing 100 U/mL of IL-1β, 1000 U/mL of tumor necrosis factor–α, and 1000 U/mL of interferon-γ, as assessed using both the tetramethylrhodamine ethyl ester assay and the colorimetric methyl tetrazolium salt Cell Titer 96 Aqueous One Solution cell proliferation assay (Promega Corp, Madison, Wisconsin). Future experiments will be required to further confirm the role of c-FLIP$_L$ expression in pig islet cells.

REFERENCES

1. Shapiro AM, Ricordi C, Hering BJ, et al: International trial of the Edmonton protocol for islet transplantation. N Engl J Med 355:1318, 2006

2. Kues WA, Niemann H: The contribution of farm animals to human health. Trends Biotechnol 22:286, 2004

3. Yi S, Feng X, Hawthorne W, et al: CD8+ T cells are capable of rejecting pancreatic islet xenografts. Transplantation 70:896, 2000

4. Tanemura M, Chong AS, DiSesa VJ, et al: Direct killing of xenograft cells by CD8+ T cells of discordant xenograft recipients. Transplantation 74:1587, 2002

5. Kawamoto K, Tanemura M, Ito T, et al: Significant inhibition of human CD8$^+$ cytotoxic T lymphocyte–mediated xenocytotoxicity by overexpression of the human decoy Fas antigen. Transplantation 81:789, 2006

6. Tanemura M, Saga A, Kawamoto K, et al: In vitro and in vivo prevention of human CD8$^+$ CTL-mediated xenocytotoxicity by pig c-FLIP expression in porcine endothelial cells. Am J Transplant 8:288, 2008

7. Irmler M, Thome M, Hahne M, et al: Inhibition of death receptor signals by cellular FLIP. Nature 388:190, 1997

8. Thome M, Schneider P, Hofmann K: Viral FLICE-inhibitory proteins (FLIPs) prevent apoptosis induced by death receptors. Nature 386:517, 1997

9. Goto Y, Matsuda-Minehata F, Inoue N, et al: Porcine (*Sus scrofa*) cellular FLICE-like inhibitory protein (cFLIP): molecular cloning and comparison with the human and murine cFLIP. J Reprod Dev 50:549, 2004

10. Ricordi C, Finke EH, Lacy PE: A method for the mass isolation of islets from the adult pig pancreas. Diabetes 35:649, 1986

11. Noguchi H, Iwanaga Y, Okitsu T, et al: Evaluation of islet transplantation from non–heart beating donors. Am J Transplant 6:2476, 2006

12. Kanegae Y, Makimura M, Saito I: A simple and efficient method for purification of infectious recombinant adenovirus. Jpn J Med Sci Biol 47:157, 1994

13. Kawamoto K, Tanemura M, Komoda H, et al: Adenoviral-mediated overexpression of membrane-bound human FasL and human decoy Fas protect pig islets against human CD8+ CTL-mediated cytotoxicity. Transplant Proc 38:3286, 2006

14. Kawamoto K, Tanemura M, Saga A, et al: Adenoviral-mediated overexpression of either membrane-bound human FasL or human decoy Fas can prolong pig islet xenograft survival in a rat transplant model. Transplant Proc 40:477, 2008

15. Bennet W, Björkland A, Sundberg B, et al: Expression of complement regulatory proteins on islets of Langerhans: a comparison between human islets and islets isolated from normal and hDAF transgenic pigs. Transplantation 72:312, 2001

16. Cardozo AK, Proost P, Gysemans C, et al: IL-1beta and IFN-gamma induce the expression of diverse chemokines and IL-15 in human and rat pancreatic islet cells, and in islets from pre-diabetic NOD mice. Diabetologia 46:255, 2003

Ann Surg Oncol (2009) 16:2035–2041
DOI 10.1245/s10434-009-0465-x

Annals of
SURGICAL ONCOLOGY
OFFICIAL JOURNAL OF THE SOCIETY OF SURGICAL ONCOLOGY

ORIGINAL ARTICLE – TRANSLATIONAL RESEARCH AND BIOMARKERS

Preoperative *u-PAR* Gene Expression in Bone Marrow Indicates the Potential Power of Recurrence in Breast Cancer Cases

Koshi Mimori, MD, PhD[1], Akemi Kataoka, MD, PhD[1], Hiroshi Yamaguchi, MD, PhD[2], Norikazu Masuda, MD, PhD[3], Yoshimasa Kosaka, MD, PhD[1], Hideshi Ishii, MD, PhD[1], Shinji Ohno, MD, PhD[2], and Masaki Mori, MD, PhD, FACS[1]

[1]Department of Surgical Oncology, Medical Institute of Bioregulation, Kyushu University, Beppu, Japan
[2]Department of Breast Oncology, Kyushu Cancer Center, Fukuoka, Japan; [3]Osaka National Hospital, Osaka, Japan

ABSTRACT

Introduction. The clinical significance of isolated tumor cells (ITC) in peripheral blood (PB) and bone marrow (BM) as predictive markers in the recurrence or metastasis of breast cancer has not yet been determined. In the current study, we focused on the *urokinase plasminogen activator receptor* (*u-PAR*) gene as a powerful indicator of the potential to relapse after surgery.

Patients and Methods. We examined *CK-7* and *CK19* as an ITC marker and *u-PAR* as a candidate indicator for metastasis in PB and BM from 800 cases of breast cancer by quantitative real-time reverse-transcription polymerase chain reaction (RT-PCR). Serum tumor markers, carcinoembryonic antigen (CEA) and cancer antigen 15-3 (CA15-3), were compared with *u-PAR* or *CK* status.

Results. *CK7* in PB was positive in 262 cases that showed a poorer disease-free survival (DFS) than 478 *CK7(–)* cases ($P < 0.05$). The 153 cases of *u-PAR*(+) in BM showed significantly poorer DFS and overall survival (OS) than did the 579 cases of *u-PAR*(–) in BM ($P < 0001$ and $P < 0.0001$, respectively). In PB, a significant difference was also observed between 330 cases of *u-PAR*(+) and 437 cases of *u-PAR*(–) ($P < 0.0001$). The hazard ratio (HR) for prediction of recurrence was significantly higher in *u-PAR* ($P < 0.0001$; HR 0.0519) than the level of three serum tumor markers.

Discussion. *u-PAR* expresses in cancer cells during the dormant phase. The current findings revealed that the expression levels of *u-PAR* in PB and BM evaluated preoperatively indicate the potential to relapse or metastasize after surgery.

First Received: 1 October 2008;
Published Online: 30 April 2009

M. Mori, MD, PhD, FACS
e-mail: mmori@gesurg.med.osaka-u.ac.jp

During the past two decades the presence of isolated tumor cells (ITC) has been determined; however, the clinical relevance to predict disease-free survival (DFS) or overall survival (OS) in patients of gastrointestinal tract cancer and breast cancer has not been determined.[1–6] Therefore, the current methodology to identify ITC does not apply to practical clinical usage at present. Why can we not use this method to predict DFS or OS more frequently than the conventional clinicopathological diagnosis? We concluded that there are problems with inadequate numbers of examined cases and a diversity of methodologies among institutes, such as target organs, target molecules, and assay systems.

Therefore, we collected both BM and PB from 800 cases of breast cancer in the Kyushu Cancer Center. This is the largest number of examined cases at a single institute in the world among published papers, except the immunohistochemical study by Braun et al.[2,7] As target genes, we chose genes that express specifically in epithelial cells in PB and BM in breast cancer. Among them, we examined *CK7* and *CK19* as candidate markers to detect ITC in breast cancer according to our previous work, which indicated that *CK7* had the best sensitivity as well as the best specificity.[8] Quantitative real-time reverse-transcription polymerase chain reaction (RT-PCR) with primers and hybridization probe enabled us to achieve the highest specificity and fidelity.

Moreover, according to a previous study by Heiss et al., *u-PAR* expression on disseminated tumor cells detected by immunocytochemistry was significantly and clearly correlated with increasing tumor cell counts and clinical

prognosis.[9] Therefore, we decided to apply the *u-PAR* gene as another target gene in PB and BM from breast cancer cases to predict recurrence and metastasis. Recent studies have focused on dormant cancer cells in BM or PB as the prospective cause for the reemergence of cancer cells after several years.[10–12] With respect to tumor dormancy and recurrence, the *u-PAR* gene encodes one of the cell surface markers that is established as one of the tumor dormancy-related markers.[13] Therefore, we evaluated the role of *u-PAR* in PB and BM as a major indicator to predict recurrence and prognosis of breast cancer cases by measuring preoperatively.

Furthermore, the large number of examined cases allowed us to evaluate the controversial conclusion of whether ITC in PB and BM can be a powerful clinical indicator to predict recurrence and prognosis. In addition, we reveal that *u-PAR* in PB and BM was a correlative marker of recurrence of breast cancer cases beyond the ITC markers as well as existing serum tumor markers.

MATERIALS AND METHODS

Bone Marrow and Peripheral Blood from Breast Cancer Cases

We examined 800 cases of breast cancer from the National Kyushu Cancer Center. Clinicopathologic variables in all cases are presented in Table 1 to determine the

TABLE 1 Clinicopathologic significance of u-PAR status in bone marrow and peripheral blood from breast cancer cases

	n	Bone marrow		*P* value	*n*	Peripheral blood		*P* value
		Positive	Negative			Positive	Negative	
	732	153	579		767	330	437	
Tumor				<0.0001				0.0006
Small	342	49	293		362	132	230	
Large	390	104	286		405	198	207	
Lymph node metastasis				ns				Ns
Positive	266	58	208		282	121	161	
Negative	466	95	371		485	209	276	
Metastasis				ns				ns
Positive	13	3	10		13	4	9	
Negative	719	150	569		754	326	428	
Histology				ns				ns
DCIS	45	10	35		47	23	24	
IDC	636	132	504		664	277	387	
Others	51	11	40		56	30	26	
Stage				ns				ns
0	14	1	13		14	6	8	
1	250	40	210		255	95	159	
2A	256	54	202		285	127	158	
2B	152	40	112		153	75	78	
3A	39	11	28		41	19	22	
3B	10	4	6		9	5	4	
4	11	3	8		10	2	8	
ER or PgR				ns				ns
Positive	556	110	446		579	244	335	
Negative	175	43	132		187	85	102	
Unknown	1	1	0		1	1	0	
HER2/Neu				ns				0.0047[a]
Positive	175	29	146		194	69	125	
Negative	360	66	294		392	188	204	
unknown	197	58	139		181	73	108	

ER estrogen receptor, *PgR* progesterone receptor, *DCIS* ductal carcinoma in situ, *IDC* invasive ductal carcinoma, ns nonsignficant

[a] HER2/neu positive cases indicated significantly higher incidence of u-PAR negative in peripheral blood

relationship between those factors and *u-PAR* status in bone marrow as well as that in peripheral blood. In brief, for analysis of bone marrow, 732 cases were eligible for further study, while 68 cases were excluded because of insufficient amounts of RNA and/or inadequate follow-up data. In 767 cases *u-PAR* was examined in peripheral blood, while 33 cases were excluded by the quality of RNA and inadequate follow-up data.

Both PB and BM were also collected from 29 cases of no malignancy that consisted of 20 cases of cholecystolithiasis, 3 cases of common bile duct stone, and 6 cases of incisional hernia to be used as the negative control from April 2000 to March 2003. After analysis of those 29 nonmalignant cases, no case was affected by cancer. Ethical committee approval for this project from Kyushu University and the National Cancer Center was obtained, and documented informed consent was obtained from all patients and control cases.

RNA Extraction

Total RNA was extracted from bone marrow and peripheral blood from the above clinical samples, for a total of PB and BM from 800 cases. Detailed procedures were described elsewhere.[14] In brief, BM was aspirated from the sternum of patients before the operation under general anesthesia. We discarded the first 1.0 ml of BM and PB to avoid contamination from the epithelial tissue of skin at the site, and collected a second 1.0 ml of BM and PB into 4.0 ml Isogen-LS (Nippon Gene, Toyama, Japan), and total RNA was extracted according to the manufacturer's protocol.

Primers and Probes for Quantitative Real-Time RT-PCR

The reverse-transcriptase reaction was performed as in our previous study.[8] In brief, first-strand cDNA was synthesized from 2.7 μg total RNA in 30 μl reaction mixture containing 5 μl 5 × RT buffer (GIBCO BRL, Gaithersburg, MD), 200 μM deoxyribonucleotide triphosphate (dNTP), 100 μM solution of random hexa-deoxynucleotide mixture, 50 units Rnasin (Promega, Madison, WI), 2 μl 0.1 M dithiothreitol, and 100 units Moloney leukemia virus RT (GIBCO BRL, Gaithersburg, MD). The mixture was incubated at 37°C for 60 min, heated to 95°C for 10 min, and then chilled on ice.

We performed real-time quantitative RT-PCR using a LightCycler instrument (Roche Diagnostics, Manheim, Germany) with the following target genes to detect ITC in PB and/or BM: *CK7*, primers: sense; 5′-ACA TCA AGA ACC AGC GTG CC-3′, antisense; 5′-TCA CGG CTC CCA CTC CAT CT-3′ and probes: donor; 5′-TGA GCG TGA AGC TGG CCC TGG ACA TCG A-fluorescein-3′ and acceptor; 5′-LCRed640- ATC GCC ACC TAC CGC AAG CTG CTG GAG G-3′-phosphorylated. *CK19*, primers: sense; 5′-AAG GTG GAT TCC GCT CCG GGC A-3′, antisense; 5′-ATC TTC CTG TCC CTC GAG CA-3′ and probes: donor; 5′-TTC AAT TCT TCA GTC CGG CTG G-fluorescein-3′ and acceptor; 5′-LCRed640- GAA CCA GGC TTC AGC ATC CTT C 3′-phosphorylated; *urokinase plasminogen activator receptor* (*u-PAR*), primers: sense; 5′-TGA ATC AAT GTC TGG TAG C-3′, antisense; 5′-TGG TTA CAG CCA CTT TTA GT-3′, and probes: donor; 5′-GCT ATA TGG TAA GAG GCT GTG CAA CCG CCT-3′-fluorescein and acceptor; 5′-LCRed640-AAT GTG CCA ACA TGC CCA CCT GGG T-3′-phosphorylated. We utilized glyceraldehyde-3-phosphate-dehydrogenase (GAPDH) as an internal control; primer: sense; 5′-TGA ACG GGA AGC TCA CTG G-3′, antisense; 5′-TCC ACC ACC CTG TTG CTG TA-3′, and probe: donor; 5′-GAG TGG GTG TCG CTG TTG AAG TCA-3′-fluorescein, acceptor; 5′-LCRed640-AGG AGA CCA CCT GGT GCT CAG TGT A-3′-phosphorylated. All primers and probes were synthesized and purified by reverse-phase high-performance liquid chromatography and the optimal reagent concentrations and PCR cycling conditions were established. Each run of RT-PCR reaction included positive controls synthesized from plasmids by the Nippon Gene Research Laboratories (Sendai, Japan).

Quatitated RT-PCR Condition

The amplification of the *u-PAR* profile consisted of one cycle at 95°C for 10 min (denaturation) followed by 40 cycles of 95°C for 10 s, 62°C for 15 s, and 72°C for 8 s. For amplification of *GAPDH*, an initial denaturation at 95°C for 10 min was followed by 15 s at 95°C, 15 s at 60°C, and 13 s at 72°C. For *CEA* amplification, an initial denaturation was also followed by 15 s at 95°C, 15 s at 56°C, and 11 s at 72°C. All experiments were performed two times to confirm reproducibility. If the second result was greater than two times or less than 50% of the first one, we performed a third experiment. Then, we calculated the average using two accepted data.

Statistical Analysis

Clinicopathologic significance of *u-PAR* expression was evaluated using Student's *t*-test. To analyze disease-free and overall survival, log-rank (Mantel–Cox) analysis was performed on *CK7*, *CK19*, and *u-PAR* in BM and PB, as well as on serum tumor markers. All tests were analyzed using JMP software (SAS Institute Inc., Cary, NC, USA). Statistical significance was determined as *P*-value from two-sided tests of less than 0.05.

RESULTS

Clinicopathologic Significance of u-PAR in Bone Marrow and Peripheral Blood

In the BM analysis in Table 1 (left side), there was a significant association between tumor size and *u-PAR* expression. We divided the tumors into two subgroups based on size: 342 cases were small tumors (Tis and T1) and 390 cases were large (T2, T3, and T4). Incidence of *u-PAR*-positive expression in bone marrow was significantly higher in cases with large tumor size ($P < 0.0001$).

In the PB analysis in Table 1 (right side), a statistically significantly higher incidence of *u-PAR*-positive expression was observed in 405 cases of large tumor size ($P = 0.0006$). It is intriguing that the human epidermal growth receptor 2 (HER2)/neu-negative cases showed a higher incidence of *u-PAR*-positive cases ($P = 0.0047$); however, there was no relationship between *u-PAR* expression and any clinicopathologic factor.

Prognostic Value of CK7 and u-PAR to Predict Disease-Free Survival

In Fig. 1, the 262 cases of *CK7*(+) in PB showed significantly worse prognosis than the 478 cases of *CK7*(–). However, a significant difference between *CK7*(+) and *CK7*(–) was observed only in the cases free of lymph node metastasis after 1 year ($P < 0.05$). On the other hand, *CK19*(+) in BM was found in 213 out of 750 cases, while *CK19*(+) in PB was found in 135 out of 750 cases; however, there was no clinical relevance of *CK19* expression in PB or in BM (data not shown).

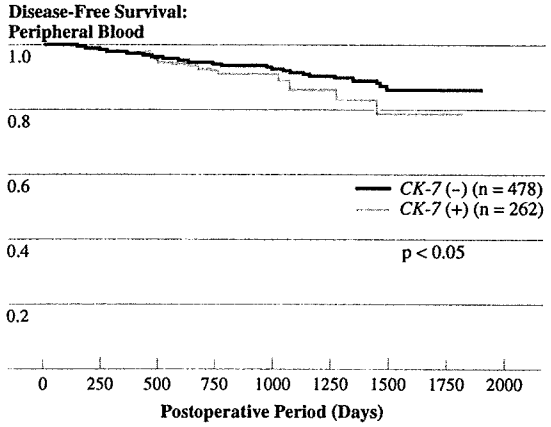

FIG. 1 Clinical relevance of cytokeratin 7 (*CK7*) gene expression and disease- free survival rate in breast cancer cases. There were significant differences between the 262 cases of *CK7*(+) and the 478 cases of *CK7*(–); however, this was observed only if restricted to cases free of lymph node metastasis after 1 year has passed ($P < 0.05$)

Disease-free survival (DFS) rate was remarkably different between *u-PAR*(+) and *u-PAR*(–) in BM and PB. In BM, disease-free survival rate was significantly worse in 153 cases of *u-PAR*(+) than in 557 cases of *u-PAR*(–) (Fig. 2a; $P < 0.0001$). In PB, 327 cases of *u-PAR*(+) showed significantly worse disease-free survival rate compared with 418 cases of *u-PAR*(–) (Fig. 2b). However, overall survival (OS) rate in BM was significantly poorer in 153 cases of *u-PAR*(+) than it was in 557 cases of *u-PAR* (–) (Fig. 3a; $P < 0.001$). In PB, *u-PAR*(+) had poorer OS than 418 cases of *u-PAR*(–); however, there was no significant difference between them (Fig. 3b).

Additionally, we combined the data of *u-PAR* and *CK* gene expression. As a result, in BM, *u-PAR*(+)/*CK*(+) showed the highest recurrence rate; however, *u-PAR* status alone was adequate to predict recurrence compared with the combined data.

Comparison with Serum Tumor Markers

We examined preoperative serum tumor markers, carcinoembryonic antigen (CEA) and cancer antigen (CA15-3), just prior to surgery in 695 and 682 cases of breast cancer, respectively (Fig. 4). We divided the value of serum tumor marker into high and low by the standard value at our hospital in each marker, i.e., 5.0 ng/ml for CEA and 7.0 U/ml for CA15-3. As shown in Fig. 4, 39 cases of high serum CEA level had much poorer DFS rate than 656 cases of low CEA level; however, there was no statistical significance between them. We could not find any clinical usefulness in serum CA15-3 levels measured just prior to surgery in breast cancer cases.

DISCUSSION

The initial purpose of the current study was to attempt to answer the controversial issue of whether or not isolated tumor cells in BM and PB have clinical significance in predicting OS and DFS. Therefore, we collected them from large numbers of breast cancer cases. We then performed quantitative RT-PCR with primers and probes to evaluate gene expression objectively and precisely compared with previous studies using immunocytological analysis. As a result, we observed a significantly higher incidence of *CK7* in PB from 740 cases of breast cancer; however, the difference of expression levels between *CK7*(+) and *CK7*(–) was inadequate to apply the evaluation of ITC (*CK7*) expression in PB to predict DFS. Additionally, we could not find any clinical relevance for predicting OS by the evaluation of ITC in PB, and ITC in BM was not associated with clinicopathologic significance in breast cancer cases. Therefore, we urgently have to identify new indicators to

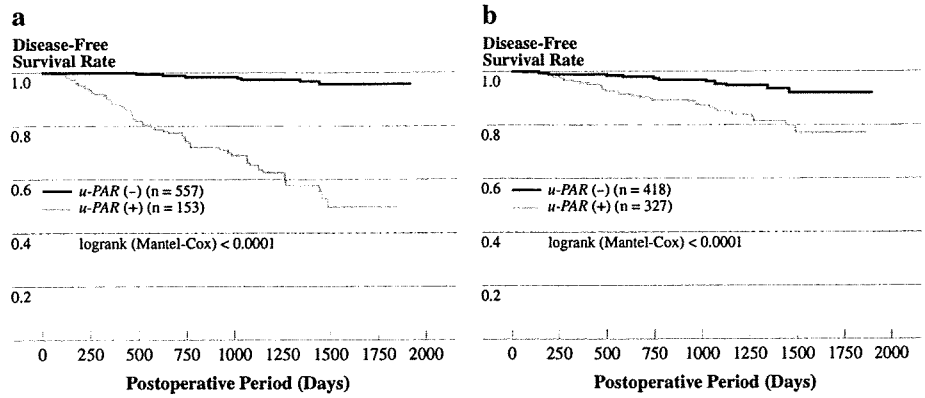

FIG. 2 Clinical significance of u-PAR gene expression in breast cancer cases. **a** Disease-free survival rate was significantly poorer in 153 cases of *u-PAR*(+) than in 557 cases of *u-PAR*(–) in bone marrow ($P < 0.0001$). **b** In peripheral blood, 327 cases of *u-PAR*(+) expression also showed significantly worse disease-free survival rate than 418 cases of *u-PAR*(–) expression ($P < 0.0001$)

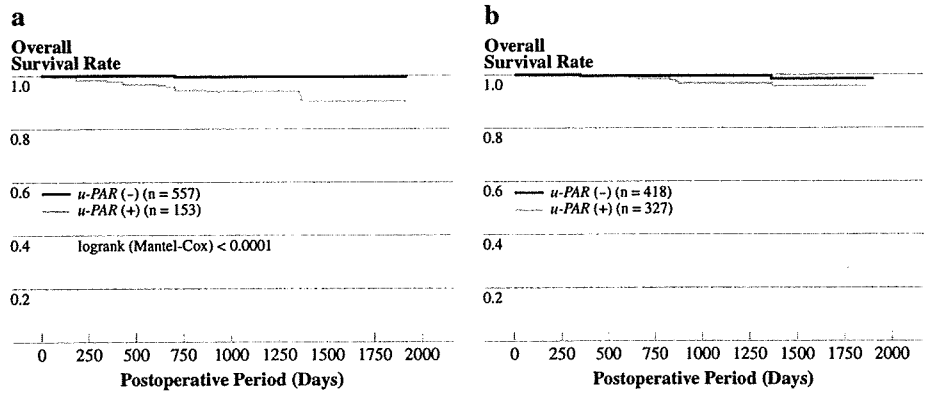

FIG. 3 Clinical significance of *u-PAR* gene expression in predicting overall survival rate (OS). **a** Significantly poorer prognosis was observed in 153 cases of *u-PAR*-positive expression than in 557 cases of *u-PAR*-negative expression in bone marrow ($P < 0.001$). **b** There was no significant difference in *u-PAR* gene status expression in peripheral blood from breast cancer cases

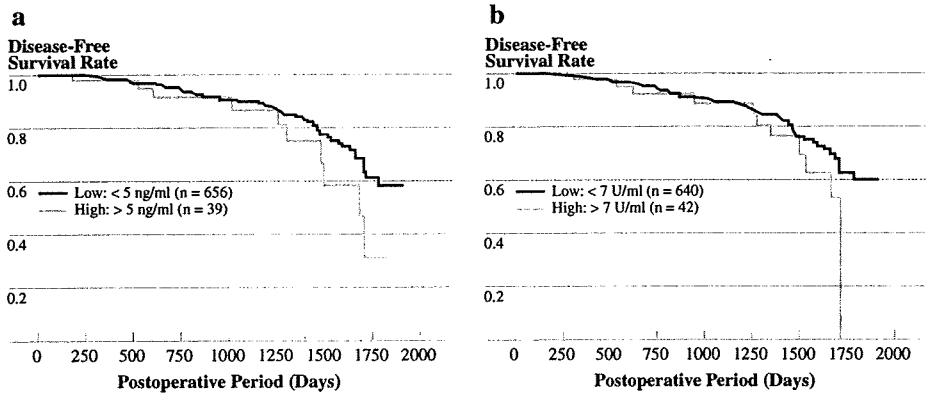

FIG. 4 Comparison of disease-free survival rate between serum tumor marker positive and negative cases by preoperative examination. **a** The cutoff value of preoperative serum CEA is 5.0 ng/ml; 656 cases of low CEA showed lower incidence of recurrence than 39 cases of high CEA; however, this difference was not significant. **b** Serum levels of preoperative CA15-3 were divided into two groups by 7.0 U/ml, yielding 42 cases of high level and 640 cases of low level; however, there was no significant difference in CA15-3 levels

predict DFS and OS in PB and BM from breast cancer cases instead of the identification of ITC.

We disclosed the distinctive clinical significance of *u-PAR* as an important recurrent marker of breast cancer cases, and also found an intriguing inverse relationship between *u-PAR* and HER2/neu expression in peripheral blood just prior to surgery. Considering the intimate relationship between u-PAR and tumor dormancy as in

previous studies, we believed that *u-PAR*-overexpressing cells in the current study were originally from abundant cancer cells at the dormant phase without upregulated cellular activity as characterized by HER2/neu protein expression.[13,15–18] Besides, several studies recently described the role of *u-PAR* gene as a tumor dormancy marker.[19,20] Allgayer et al. mentioned that u-PAR is a key player in regulating the shift between single-cell tumor dormancy and proliferation, and they concluded that u-PAR might be an essential molecule in bone marrow disseminated tumor cells for long-term survival during dormancy, and/or reactivation of their proliferation years after primary treatment.[21] Therefore, the current study can be an initial one to show the role of u-PAR as an indicator of disseminated tumor cells for long-term survival during dormancy on a large scale for breast cancer cases. Besides, larger size of tumor showed positive expression of *u-PAR* in peripheral blood and bone marrow. We assumed that higher population of *u-PAR*-expressing cells must be present in larger-size tumors, worsening the relapse-free survival rate (Fig. 2) and overall survival rate (Fig. 3).

Furthermore, regarding the origins of the *u-PAR* gene, we supposed the following two possibilities: from cancer cells in the dormant phase as described above, or originated from the tumor-bearing host. In addition to our recent study, several previous studies disclosed that metastasis and/or recurrence in solid cancer was generated by the presence of host-side factors, such as cytokines, chemokines, and "niche cells" working with possible cancer stem cells, hematopoietic progenitor cells (HPC), circulating endothelial cells (CEC), mature endothelial cells, tumor vessels, endothelial progenitor cells, and inflammatory cytokines, such as interleukin (IL)-10 and IL-12 *R*.[22–27] In the current study, an RT-PCR assay should have detected *u-PAR*-expressing cells among the highly populated and enriched cells in blood; however, further study is required to determine the origin of *u-PAR*-gene-expressing cells in PB and BM.

Considering clinical application of *u-PAR*, we found the significant magnitude of *u-PAR* gene in the prediction of DFS as well as OS from peripheral blood much easier without invasion to patients rather than bone marrow. Therefore, the evaluation of expression of *u-PAR* gene status will be available at the outpatient clinic.

In conclusion, we predicted cancer recurrence by evaluating *u-PAR* expression rather than looking for the existence of cancer cells (*CK7*) in the circulating system. The origin of *u-PAR* expression remains unknown; however, the most intriguing matter relevant to patients is that measurement of *u-PAR* gene by RT-PCR can be applied clinically to predict recurrence and overall survival instead of those serum tumor markers preoperatively. The current finding enabled us to select patients to be treated with adjuvant chemotherapy in addition to the criteria for the standard breast cancer treatment.

ACKNOWLEDGEMENT This work was supported by the following grant sponsors: CREST, Japan Science and Technology Agency (JST); Japan Society for the Promotion of Science (JSPS) Grant-in-Aid for Scientific Research, grant numbers 17109013, 17591411, 17591413, 18390367, 18590333, 18659384, and 18790964; The Ministry of Education, Culture, Sports, Science, and Technology (MEXT) Grant-in-Aid for Scientific Research on Priority Areas, grant number 18015039; and the Third Term Comprehensive Ten-Year Strategy for Cancer Control, grant number 16271201.

REFERENCES

1. Braun S, Cevatli BS, Assemi C, Janni W, Kentenich CR, Schindlbeck C, et al. Comparative analysis of micrometastasis to the bone marrow and lymph nodes of node-negative breast cancer patients receiving no adjuvant therapy. *J Clin Oncol.* 2001;19: 1468–75.
2. Braun S, Pantel K, Muller P, et al. Cytokeratin-positive cells in the bone marrow and survival of patients with stage I, II, or III breast cancer. *New Eng J Med.* 2000;342:525–33.
3. Mansi JL, Gogas H, Bliss JM, Gazet JC, Berger U, Coombes RC. Outcome of primary-breast-cancer patients with micrometastases: a long-term follow-up study. *Lancet.* 1999;354:197–202.
4. Masuda N, Tamaki Y, Sakita I, et al. Clinical significance of micrometastases in axillary lymph nodes assessed by reverse transcription-polymerase chain reaction in breast cancer patients. *Clin Cancer Res.* 2000;6:4176–85.
5. Molino A, Micciolo R, Turazza M, et al. Prognostic significance of estrogen receptors in 405 primary breast cancers: a comparison of immunohistochemical and biochemical methods. *Breast Cancer Res Treat.* 1997;45:241–9.
6. Salvadori B, Squicciarini P, Rovini D, et al. Use of monoclonal antibody MBr1 to detect micrometastases in bone marrow specimens of breast cancer patients. *Eur J Cancer.* 1990;26:865–7.
7. Braun S, Vogl FD, Naume B, et al. A pooled analysis of bone marrow micrometastasis in breast cancer. *New Eng J Med.* 2005; 353:793–802.
8. Masuda TA, Kataoka A, Ohno S, et al. Detection of occult cancer cells in peripheral blood and bone marrow by quantitative RT-PCR assay for cytokeratin-7 in breast cancer patients. *Int J Oncol.* 2005;26:721–30.
9. Heiss MM, Allgayer H, Gruetzner KU, et al. Individual development and uPA-receptor expression of disseminated tumour cells in bone marrow: a reference to early systemic disease in solid cancer. *Nat Med.* 1995;1:1035–9.
10. Allan AL, Vantyghem SA, Tuck AB, Chambers AF. Tumor dormancy and cancer stem cells: implications for the biology and treatment of breast cancer metastasis. *Breast Dis.* 2006;26:87–98.
11. Brackstone M, Townson JL, Chambers AF. Tumour dormancy in breast cancer: an update. *Breast Cancer Res.* 2007;9:208.
12. Demicheli R, Retsky MW, Hrushesky WJ, Baum M. Tumor dormancy and surgery-driven interruption of dormancy in breast cancer: learning from failures. *Nat Clin Pract Oncol.* 2007;4: 699–710.
13. Laufs S, Schumacher J, Allgayer H. Urokinase-receptor (u-PAR): an essential player in multiple games of cancer: a review on its role in tumor progression, invasion, metastasis, proliferation/ dormancy, clinical outcome and minimal residual disease. *Cell Cycle. Georgetown, Tex* 2006;5:1760–71.
14. Iinuma H, Okinaga K, Egami H, et al. Usefulness and clinical significance of quantitative real-time RT-PCR to detect isolated

tumor cells in the peripheral blood and tumor drainage blood of patients with colorectal cancer. *Int J Oncol.* 2006;28:297–306.
15. Holmgren L, O'Reilly M, Folkman J. Dormancy of micrometastases: Balanced proliferation and apoptosis in the presence of angiogenesis suppression. *Nat Med.* 1995;1:149–53.
16. Murray C. Tumour dormancy: not so sleepy after all. *Nat Med.* 1995;1:117–8.
17. Pantel K, Brakenhoff R Dissecting the metastatic cascade. *Nat Rev Cancer.* 2004;4:448–56.
18. Uhr J, Scheuermann R, Street N, Vitetta E. Cancer dormancy: opportunities for new therapeutic approaches. *Nat Med.* 1997;3: 505–9.
19. Riethdorf S, Wikman H, Pantel K. Review: biological relevance of disseminated tumor cells in cancer patients. *Int J Oncol.* 2008; 123:1991–2006.
20. Wikman H, Vessella R, Pantel K. Cancer micrometastasis and tumour dormancy. *Apmis.* 2008;116:754–70.
21. Allgayer H, Aguirre-Ghiso JA. The urokinase receptor (u-PAR)–a link between tumor cell dormancy and minimal residual disease in bone marrow? *Apmis.* 2008;116:602–14.
22. Mimori K, Fukagawa T, Kosaka Y, et al. Hematogenous metastasis in gastric cancer requires isolated tumor cells and expression of vascular endothelial growth factor receptor-1. *Clin Cancer Res.* 2008;14:2609–16.
23. Peters BA, Diaz LA, Polyak K, et al. Contribution of bone marrow-derived endothelial cells to human tumor vasculature. *Nat Med.* 2005;11:261–2.
24. Hildenbrand R, Glienke W, Magdolen V, Graeff H, Stutte HJ, Schmitt M. Urokinase receptor localization in breast cancer and benign lesions assessed by in situ hybridization and immunohistochemistry. *Histochem Cell Biol.* 1998;110:27–32.
25. Schlimok G, Funke I, Pantel K, et al. Micrometastatic tumour cells in bone marrow of patients with gastric cancer: methodological aspects of detection and prognostic significance. *Eur J Cancer.* 1991;27:1461–5.
26. Dubuisson L, Monvoisin A, Nielsen BS, Le Bail B, Bioulac-Sage P, Rosenbaum J. Expression and cellular localization of the urokinase-type plasminogen activator and its receptor in human hepatocellular carcinoma. *J Pathol.* 2000;190:190–5.
27. Pyke C, Graem N, Ralfkiaer E, et al. Receptor for urokinase is present in tumor-associated macrophages in ductal breast carcinoma. *Cancer Res.* 1993;53:1911–5.

OPEN ACCESS Freely available online

PLoS one

Dicer Is Required for Maintaining Adult Pancreas

Sumiyo Morita[1,2], Akemi Hara[3], Itaru Kojima[3], Takuro Horii[1], Mika Kimura[1,2], Tadahiro Kitamura[4], Takahiro Ochiya[5], Katsumi Nakanishi[6], Ryo Matoba[6], Kenichi Matsubara[6], Izuho Hatada[1]*

1 Laboratory of Genome Science, Biosignal Genome Resource Center, Institute for Molecular and Cellular Regulation, Gunma University, Showa-machi Maebashi, Japan, 2 Japan Health Sciences Foundation, Chuo, Tokyo, Japan, 3 Department of Molecular Medicine, Institute for Molecular and Cellular Regulation, Gunma University, Showa-machi Maebashi, Japan, 4 Metabolic Signal Research Center Laboratory of Metabolic Signal, Institute for Molecular and Cellular Regulation, Gunma University, Showa-machi Maebashi, Japan, 5 National Cancer Center Research Institute, Section for Studies on Metastasis, Tsukiji, Chuo-ku, Tokyo, Japan, 6 DNA Chip Research Inc., Suehirocho, Tsurumi-ku, Yokohama, Japan

Abstract

Dicer1, an essential component of RNA interference and the microRNA pathway, has many important roles in the morphogenesis of developing tissues. *Dicer1* null mice have been reported to die at E7.5; therefore it is impossible to study its function in adult tissues. We previously reported that *Dicer1*-hypomorphic mice, whose *Dicer1* expression was reduced to 20% in all tissues, were unexpectedly viable. Here we analyzed these mice to ascertain whether the down-regulation of *Dicer1* expression has any influence on adult tissues. Interestingly, all tissues of adult (8–10 week old) *Dicer1*-hypomorphic mice were histologically normal except for the pancreas, whose development was normal at the fetal and neonatal stages; however, morphologic abnormalities in *Dicer1*-hypomorphic mice were detected after 4 weeks of age. This suggested that *Dicer1* is important for maintaining the adult pancreas.

Citation: Morita S, Hara A, Kojima I, Horii T, Kimura M, et al. (2009) Dicer Is Required for Maintaining Adult Pancreas. PLoS ONE 4(1): e4212. doi:10.1371/journal.pone.0004212

Editor: Kerby Shedden, University of Michigan, United States of America

Received October 22, 2008; **Accepted** December 9, 2008; **Published** January 16, 2009

Funding: This work was supported in part by the Japan Health Sciences Foundation (S.M. is a fellowship holder from the Japan Health Sciences Foundation), grants from the Ministry of Education, Culture, Sports, Science and Technology of Japan (I.H. and I.K.), the Ministry of Health, Japan Health Sciences Foundation, Labor and Welfare of Japan (T.O. and I.H.) and a grant from the Realization of Regenerative Medicine (I.K.). The funders had no role in study design, data collection and analysis, decision to publish, or preparation of the manuscript.

Competing Interests: The authors have declared that no competing interests exist.

* E-mail: ihatada@showa.gunma-u.ac.jp

Introduction

MicroRNA (miRNA) is small (~22 nucleotides), non-coding RNA. Mature miRNA transcribed as long primary transcripts is processed to pre-miRNA in the nucleus by *Drosha/DGC8* [1], and then processed in the cytoplasm by *Dicer* [2]. MiRNA is further incorporated into the RNA-inducing silencing complex (RISC), which includes Argonaute [3] to regulate gene expression via post-transcriptional repression. Over the past few years, more than 400 miRNAs have been identified, but their function is largely unknown. Several miRNAs exhibit tissue-specific or developmental stage-specific expression [4,5], indicating that they have important roles in many biological processes.

Dicer1 encodes an RNaseIII endonuclease, a key enzyme that processes miRNA. It is broadly expressed in developing tissues, and several mutant alleles of *Dicer1* have been generated in mice. *Dicer1* seems to be critical in early development since loss of its function was lethal at embryonic day 7.5 [6]. Characterization of *Dicer1* hypomorphic mice showed that the gene is required for embryonic angiogenesis [7]. Conditional inactivation of *Dicer1* in the mouse limb bud mesenchyme [8], lung epithelium [9], epidermal hair follicle [10], and pancreas [11], T cell development and differentiation [12] led to the conclusion that *Dicer1*, which processes miRNA, is indispensable for the development and morphogenesis of these tissues.

We previously generated *Dicer1*-hypomorphic mice (homozygous *Dicer1*−/− mice) [13]. Complete loss of *Dicer1* in mice results in early embryonic death [6]; however, our *Dicer1*-hypomorphic mice were viable [13]. To study the function of *Dicer1* in the maintenance of homeostasis in adult tissues, we analyzed the adult tissues histologically and found abnormalities only in the pancreas. The phenotypes detected in the pancreas of *Dicer1*-hypomorphic mice might resemble the differentiation of endocrine precursor cells in adult pancreas.

The pancreas consists of three main tissue cell types: the endocrine cells (islet of Langerhans) which produce hormones such as insulin and glucagon; the exocrine acinar tissues which secrete digestive enzymes; and the branched duct. Numerous mechanisms that control the differentiation of endocrine and exocrine cells in the embryonic pancreas have been revealed [14], but how endocrine cells (especially insulin-producing β cells) are maintained in postnatal life has been controversial [15]. At E9.5, the endocrine cells of the pancreas arise from endocrine precursor cells, which express both glucagon and insulin and divide into distinct lineages such as glucagon or insulin-expressing cells. On the other hand, in the adult pancreas, it had been considered that there are no endocrine progenitor cells and that β cells are generated only by the replication of existing β cells, not from the differentiation of endocrine precursor cells (neogenesis) [16,17]. However, several studies suggested that β cell differentiation from endocrine precursor cells can occur in adults in the regenerating pancreas after a partial pancreatectomy or duct ligation [18,19,20,21]. In the regenerating pancreas, vigorous expansion of the β cell population was observed, and partial pancreatectomy and duct ligation has been a good model for regenerating endocrine cells. The phenotypes observed in *Dicer1*-hypomorphic

mice suggested that *Dicer1* regulates the endocrinal neogenesis in the adult pancreas. Previous study showed that *Dicer1* is indispensable for normal development of the pancreas [11]; however, its function in the adult pancreas had not been elucidated. Here we report that *Dicer1* also has important functions in the adult pancreas.

Results

Dicer1 expression was significantly reduced in all tissues of *Dicer1*-hypomorphic mice but histological abnormalities were only found in the pancreas

Dicer1-hypomophic mice (homozygous *Dicer1*−/− mice) showed a lower birth rate than expected by Mendelian rules [13]; however, they did not differ from their wild-type littermates in overall health. Although they showed slight growth retardation from 10 to 50 days of age, their body weight was similar to that of wild-type mice after 50 days of age (Fig. 1). A comparison of *Dicer1* expression in nine tissues of adult mice revealed a 70–85% reduction in the hypomorphic mice (Fig. 2). Although we analyzed more than 40 tissues (Table 1), histological examination revealed no abnormalities in any tissues except the pancreas (Fig. 3); thus we focused on the pancreas of *Dicer1*-hypomorphic mice.

Dicer1 could be involved in differentiation of endocrine cells in adult pancreas

In *Dicer1*-hypomorphic mice, the size of the pancreas in adults (8–10 weeks of age) was nearly identical to that in the wild-type mice; however, there were more small islets (Fig. 4). In some of these islets, the distribution of islet cells and staining of nuclei were irregular (Fig. 5A). The boundary of islets and ducts was not clearly defined in the pancreas (Fig. 5B). Immunohistochemical analysis revealed mostly normal staining of insulin and glucagon at 8–10 weeks of age; however, the number of ductal epithelial cells stained with insulin or glucagon was significantly increased (Fig. 5C-III, P = 0.0051). In some models of pancreatic regeneration including partial pancreatectomy, insulin or glucagon-stained cells are present in the ductal epithelium, which had led to the idea that some endocrine cells differentiate in the ducts [18,19,20,21]. Our observations in *Dicer1*-hypomorphic mice suggest that regeneration from the endocrine precursor cells took

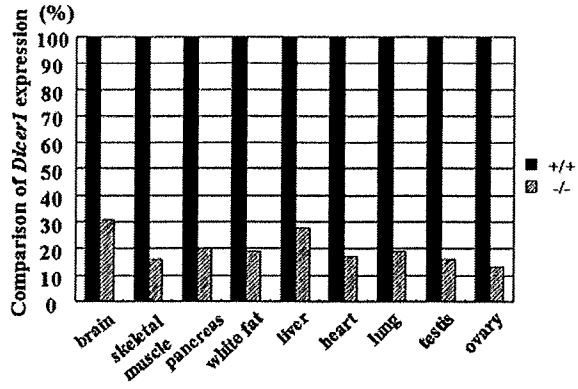

Figure 2. Comparison of *Dicer1* expression in nine tissues between wild-type (+/+) and *Dicer1*-hypomorphic (−/−) mice. The expression in the *Dicer1*-hypomorphic mice was normalized to that in the wild-type mice.
doi:10.1371/journal.pone.0004212.g002

place in adulthood. Next we conducted a histological examination of the markers Pdx-1 and Ki67. The population of ducts containing Pdx-1-positive cells was significantly increased (Fig. 5C-IV, P = 0.009). Pdx1-positive cells in the ducts are possibly the adult progenitor cells [22,23], and PDX-1 protein was detected in the pancreatic duct in adult rats after partial pancreatechtomy [21]. Surprisingly, abnormal staining of Ki67, which is a marker for proliferation of the cells, was detected in the pancreatic ducts in two of six *Dicer1*-hypomorphic mice (Fig. 5C-V). In some Ki-67-positive ducts, all the epithelial cells were stained. No such observations were found in wild-type mice.

Interestingly, cells morphologically different from either acinar or islet cells were observed in *Dicer1*-hypomorphic mice (Fig. 5D-I). Under a light microscope, some appeared to be syncytial multinucleated cells near the pancreatic duct and in acini. Numerous nuclei were distributed irregularly and were often clustered in the cells, which were all double-positive for insulin and glucagon (Fig. 5E). Cells double-positive for insulin and glucagon were significantly increased in *Dicer1*-hypomorphic mice compared to wild-type mice (Fig. 5D-II, P = 0.0019). In the exocrine portion of

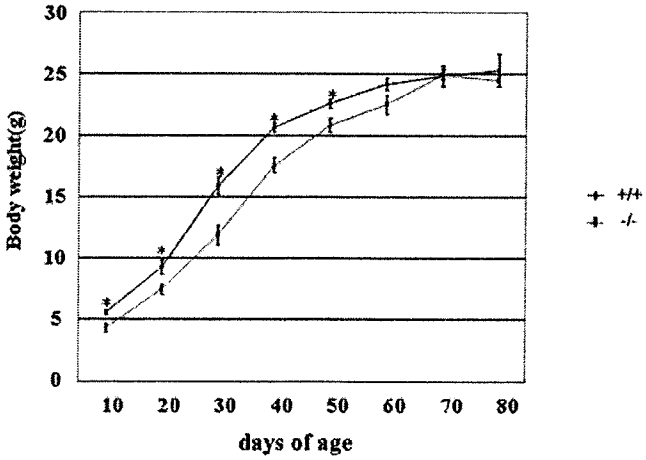

Figure 1. Body weight growth curves. Male wild-type (+/+) and *Dicer1*-hypomorphic (−/−) mice were measured to determine the change in body weight from 10 to 80 days of age. *, P<0.05. n = 8–10 per group.
doi:10.1371/journal.pone.0004212.g001

Table 1. The list of tissues with histological analysis (H&E assessment).

lung	testis	eye boll	trachea
heart	epididymis	harderian gland	esophagus
kidney	prostate	skeletal muscle	thyroid gland
pancreas	seminal vesicle	sciatic nerve	liver
tongue	coagulating gland	skin	cholecyst
stomach	bladder	breast bone	spleen
duodenum	adrenal	femur	
jejunum	pituitary gland	cerebrum	
ileum	submandibular gland	hippocampus	
cecum	parotid gland	thalamus	
colon	thymus	cerebellum	
rectum	cervical lymph node	spinal cord	

Histological analysis of these tissues was performed in wild-type (+/+) (n = 2) and *Dicer1*-hypomorphic (−/−) mice (n = 4).
doi:10.1371/journal.pone.0004212.t001

the pancreas of *Dicer1*-hypomorphic mice, most acini were morphologically normal, but some showed an irregular morphology (Fig. 5F). The shapes and position of the cells were irregular and the acinar structure was not organized. In normal acinar cells, zymogen granules are observed in the center of the acinus and the nucleus is located at its periphery.

We next investigated when the abnormal morphology appeared in the development of the pancreas in *Dicer1*-hypomorphic mice. For this purpose, a histological analysis was performed using E15.5 embryos, P1 mice, and 4-week-old mice. The pancreas of both wild-type and *Dicer1*-hypomorphic mice developed normally and endocrine and exocrine cells appeared morphologically normal at E15.5 and P1 (Fig. 6A, B); the same abnormalities observed in adult *Dicer1*-hypomorphic mice were detectable at 4 weeks of ages (Fig. 6C), although the number of abnormal cells was less than that found in adult *Dicer1*-hypomorphic mice. This suggested that the pancreas of *Dicer1*-hypomorphic mice developed normally after birth and abnormal cells appeared at around 4 weeks after birth, increasing with age.

Surprisingly, the observations found in *Dicer1*-hypomorphic mice were quite similar to the histological findings in transgenic mice expressing a truncated type II activin receptor [24]. Therefore, we next investigated the expression of the activin type II receptor in the pancreas of *Dicer1*-hypomorphic mice. Two related receptors, ActRIIA and ActRIIB, were initially identified as type II receptors for activin [25,26]. ActRIIA and ActRIIB have been reported to bind not only to activin [27], but also to other TGF-β family proteins, including BMP7 [28], GDF8 [29], Nodal [30], and GDF11 [31]. The precise role of the two activin receptors is still not clear. Real-time PCR analysis revealed that the expression of ActRIIA was slightly up-regulated in *Dicer1*-hypomorphic mice compared to wild-type mice, while the expression of ActRIIB did not differ (Fig. 7). Therefore, the abnormal morphology might be attributed to another signaling cascade.

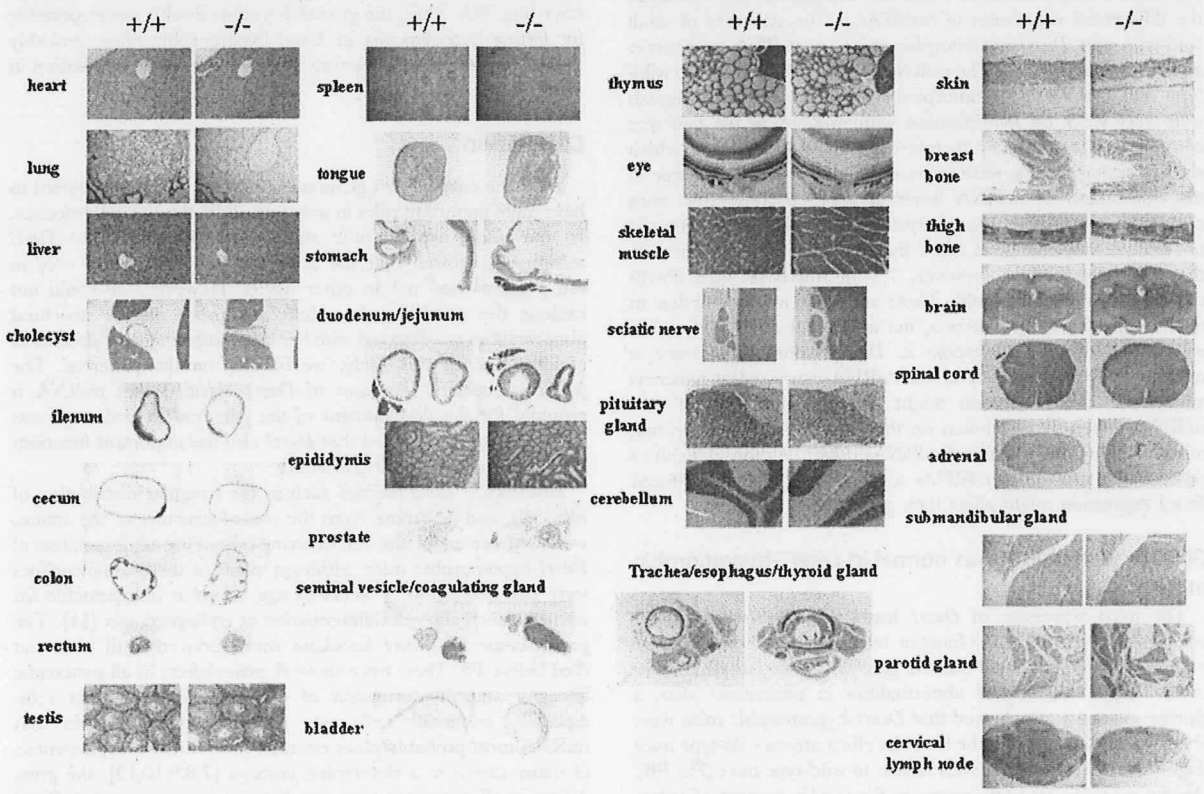

Figure 3. H&E-stained section of adult tissues of wild-type (+/+) (n = 2) and *Dicer1*-hypomorphic (−/−) mice (n = 4).
doi:10.1371/journal.pone.0004212.g003

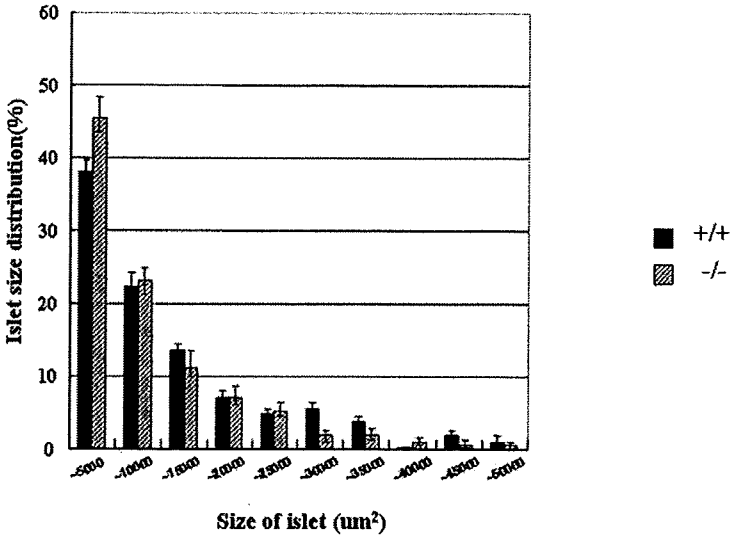

Figure 4. Comparison of the size of islets in wild-type and *Dicer1*-hypomorphic mice. The islets mass was measured in wild-type (blue bar) and *Dicer1*-hypomorphic mice (pink bar). The numbers of islets were examined in wild-type (n = 6) and *Dicer1*-hypomorphic (n = 6) mice, with six sections from each animal. The graph shows the percentage of islets in each size category.
doi:10.1371/journal.pone.0004212.g004

Detection of differential expressed miRNAs by microarray analysis

Because *Dicer1* is required for the processing of miRNAs, the reduction of *Dicer1* results in a decrease in miRNAs. To determine the differential expression of miRNAs in the pancreas of adult wild-type and *Dicer1*-hypomorphic mice, a miRNA microarray analysis was performed. The miRNAs of the pancreas of two wild-type and two *Dicer1*-hypomorphic mice were analyzed. Signals were very weak on hybridization with miRNA in the pancreas compared to other tissues; therefore a total of 83 miRNAs, which showed strong signals, were analyzed. Fig. 8 shows the change in the distribution of miRNA levels in *Dicer1*-hypomorphic mice compared to wild-type mice. Surprisingly, miRNA expression did not dramatically change in *Dicer1*-hypomorphic mice compared to the wild-type animals: however, 7% of miRNAs were down-regulated less than 0.5 fold. These miRNAs might function in maintaining the adult pancreas, but at present their relationship with the abnormal phenotype in *Dicer1*-hypomorphic mice is unclear. Why was only 7% of the miRNA expressed in pancreas attenuated? Dicer1 protein might catalyze processing of pre-miRNA differently dependent on the sequence when generating miRNA. The down-regulated miRNAs might be more difficult to process than the other miRNAs and thus significantly reduced *Dicer1* expression might affect their generation.

Glucose metabolism was normal in *Dicer1*-hypomorphic mice

The hypo-expression of *Dicer1* leads to abnormal endocrine cells, which might affect the function of the pancreas; therefore, we next investigated the metabolism of glucose in *Dicer1*-hypomorphic mice. Despite histological abnormalities in pancreatic islets, a glucose tolerance test showed that *Dicer1*-hypomorphic mice were able to clear glucose from the blood as efficiently as wild-type mice (Fig. 9A), and had insulin levels similar to wild-type mice (Fig. 9B). Despite no significant differences in the insulin content of serum after overnight fasting, *Dicer1*-hypomorphic mice showed a slightly reduced blood glucose level on fasting. *Dicer1*-hypomorphic mice were smaller than the wild-type mice before 50 days of age; therefore, we hypothesized that the growth hormone level affects fasting hypoglycemia. We checked the blood growth hormone level; however, we found no significant differences with wild-type mice (Fig. 9C). Thus, the growth hormone level is not responsible for fasting hypoglycemia in *Dicer1*-hypomorphic mice, probably due to an unknown mechanism involved in glucose metabolism in other tissues.

Discussion

Dicer, the enzyme that generates miRNAs, has been reported to have quite important roles in a variety of developmental processes. In our *Dicer1*-hypomorphic mice, histological analysis (H&E assessment) showed that the abnormalities were found only in the pancreas and not in other tissues. However, we could not exclude the possibility that there are more minute structural abnormalities not detected with the H&E assessment, or functional abnormlities. In this study, we focused on the pancreas. The pancreatic-specific knockout of *Dicer1* clarified that miRNA is required for the development of the pancreas in embryogenesis [11]. Our study suggested that *Dicer1* also has important functions in maintaining the adult pancreas.

Histological abnormalities such as the irregular distribution of islet cells, and deviations from the typical structure of the acinus, were found in endocrine and exocrine cells in the adult pancreas of *Dicer1*-hypomorphic mice, although none of these abnormalities were detected before 4 weeks of age. *Dicer1* is indispensable for normal pancreatic cell differentiation at embryogenesis [11]. The pancreas-specific *Dicer1* knockout mice survived until birth but died before P3. These mice showed gross defects in all pancreatic lineages, and the formation of exocrine cells and duct cells, especially endocrine cells, was greatly impaired. Given that miRNA most probably plays essential roles in the morphogenesis of many tissues in a developing embryo [7,8,9,10,12], the gross defects in all pancreatic lineages observed upon removal of *Dicer1* are not surprising. These mice died soon after birth; therefore, it is impossible to study the role *Dicer* may play in adult tissues.

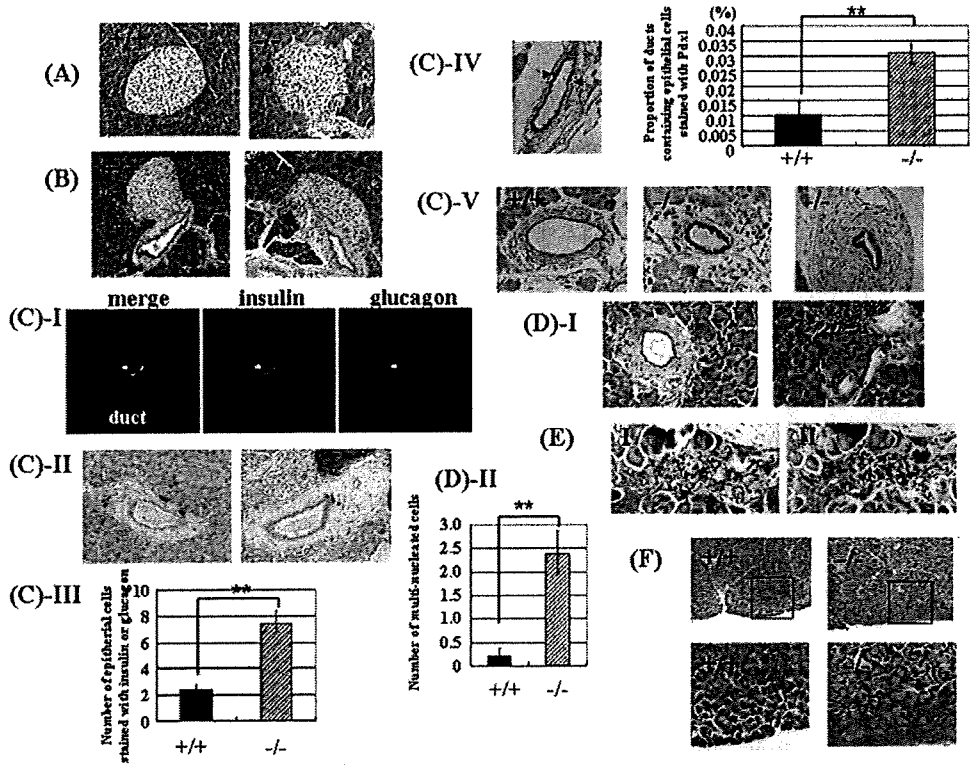

Figure 5. Pancreas morphology in adult (8–10 weeks of age) *Dicer1*-hypomorphic mice. A, B: Hematoxylin-eosin (H & E)-stained islets of the pancreas from an 8-week-old wild-type (+/+) mouse and *Dicer1*-hypomorphic (−/−) mice (*400). A: Arrows indicate an irregular distribution of islet cells. B: Arrowheads indicate that the boundary of islets and ducts was not clearly defined in the pancreas of *Dicer1*-hypomorphic mice. C: Immunohistochemistry of duct cells of *Dicer1*-hypomorphic mice. (I) Insulin (green) and glucagon (red) double-expressing cells were detected in the duct. (II) Insulin-positive cells (brown) and glucagon-positive cells (blue) were observed in the duct. (III) Comparison of the number of epithelial cells stained with both insulin and glucagon, only insulin, and only glucagon in wild-type and *Dicer1*-hypomorphic mice. These numbers were averaged from 6 animals, with six sections from each animal. **, $P<0.01$. (IV) Comparison of the proportion of ducts containing epithelial cells stained with Pdx1 in wild-type and *Dicer1*-hypomorphic mice. Arrowheads indicate the Pdx1-positive cells. *, $P<0.01$. (V) Abnormal staining of Ki67 was observed in the pancreas of *Dicer1*-hypomorphic mice. D: (I) H & E-stained multinuclear atypical cells in the pancreas of *Dicer1*-hypomorphic mice. The black dotted line indicates atypical multinuclear cells. (II) Comparison of the number of multi-nucleated cells in wild-type and *Dicer1*-hypomorphic mice. These numbers were averaged from 6 animals, with six sections from each animal. **, $P<0.01$. E: Immunohistochemistry of multinuclear atypical cells of adjacent sections of the pancreas of *Dicer1*-hypomorphic mice using anti-insulin (I) and anti-glucagon (II) antibodies. F: H & E-stained acinar cells. The rectangular areas outlined in the upper panels are magnified in the lower panels. An abnormal structure of exocrine cells was observed in the pancreas of *Dicer1*-hypomorphic mice.

doi:10.1371/journal.pone.0004212.g005

The pancreas of our *Dicer1*-hypomorphic mice developed normally and the reduced expression of *Dicer1* did not affect the development of the pancreas during embryogenesis or the neonatal stage. However, aberrant endocrine and exocrine cells could be detected after 4 weeks of age, and the number of abnormal regions seemed to increase with age. It is interesting that the developing pancreas during embryogenesis and the adult pancreas differ in sensitivity to the *Dicer1* level. In other words, the reduction in *Dicer1* only affects the maintaining of adult pancreas, not the normal development of the pancreas.

In addition, these observations, such as the increasing number of ductal epithelial cells stained positive for insulin, glucagon, and Pdx-1 in *Dicer1*-hypomorphic mice (Fig. 5D-III, IV), were also found in the regenerating pancreas [18,19,20,21], suggesting that the differentiation of endocrine precursor cells (neogenesis) occurred in the adult pancreas. Moreover, a quite intriguing observation was the existence of unknown abnormal multi-nucleated cells in the pancreas that expressed both glucagon and insulin. In the developing pancreas, endocrine precursor cells first appeared at E9, and these cells expressed both glucagon and insulin [32,33], then differentiated into insulin-producing cells or glucagon-producing cells. These cells in our adult *Dicer1*-hypomorphic mice resembled endocrine precursor cells in the fetal pancreas in terms of the expression of both glucagon and insulin. Therefore, *Dicer1* might have roles in regulating endocrine precursor cells in the adult pancreas.

The proliferation of duct cells is increased in the regenerating pancreas compared to the normal adult pancreas [20]. However, in some *Dicer1*-hypomorphic mice, abnormal proliferation of duct epithelial cells was observed (Fig. 5D-V). These features were not detected in wild-type mice and could be caused by the reduction in *Dicer1*.

Surprisingly, these histological observations in *Dicer1*-hypomorphic mice were quite similar to the histological findings in transgenic mice expressing the truncated type II activin receptor [24]. However, as our *Dicer1*-hypomorphic mice showed only a 1.2-fold increase in ActRIIA in the pancreas, ActRIIA might not cause the abnormal phenotype.

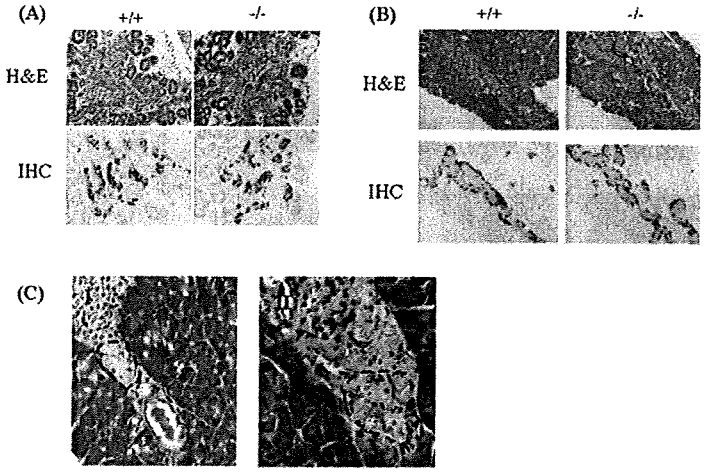

Figure 6. Histological and immunohistochemical analysis of the pancreas at E15.5 (A) and P1 (B) of wild-type and *Dicer1*-hypomorphic mice. *Dicer1*-hypomorphic mice show normal insulin (brown) and glucagon (blue) staining at E15.5 and P1. C: Histological abnormalities found in the pancreas of 4-week-old *Dicer1*-hypomorphic mice. (I) The endocrinal distribution was slightly irregular. The dotted line indicates the abnormal region of the islet. (II) Multi-nucleated cells were observed. The dotted line indicates multi-nucleated cells, which were also found in the pancreas of adult *Dicer1*-hypomorphic mice.
doi:10.1371/journal.pone.0004212.g006

Because *Dicer1* has a key role in generating a large number of miRNAs, its removal results in a significant decrease in miRNAs. In the pancreas of our *Dicer1*-hypomorphic mice, the expression levels of miRNA changed slightly compared to wild-type level which is why the mice could survive. A complete loss of *Dicer* in mice results in early embryonic death. A large number of genes control the development or maintenance of the pancreas, and these genes might be a potential target of miRNAs. Even a slight change in miRNA expression might affect the gene expression, leading to the abnormal morphology in *Dicer1*-hypomorphic mice. Further exploration is necessary to investigate the relation between these genes and miRNA in the pancreas.

Our results suggest that *Dicer1* functions in the adult pancreas and also raise the possibility that *Dicer1* regulates the differentiation of endocrine precursor cells there. Further analysis is necessary to understand the mechanism behind the maintenance of each cell type in the adult pancreas, especially β cells.

Materials and Methods

Gene targeting and mice

We generated *Dicer1*-deficient mice from an ES cell (RFF266), which was obtained from Bay Genomics [34], carrying a gene trap insertion between exon 22 and exon 23, resulting in disruption of the second RNaseIII domain and loss of the double-stranded RNA-binding domain. A gene trap vector called pGT1Lxf, which has a splicing acceptor, was used to make this ES cell. Targeted clones were injected into blastocysts to generate chimeras. Five chimeras were generated and backcrossed with

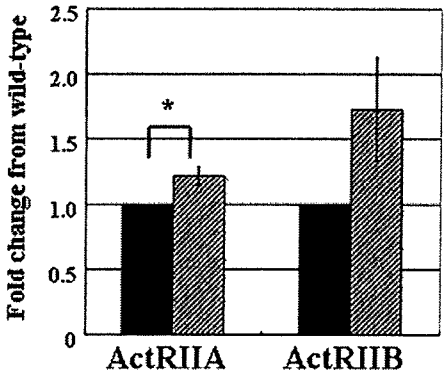

Figure 7. Analysis of ActRIIA and ActRIIB expression. Data are expressed relative (n-fold) to the wild-type pancreas and correspond to the means and standard errors for three independent experiments performed in triplicate. *, P<0.05. wild-type n = 9, *Dicer1*-hypomorphic mice n = 9.
doi:10.1371/journal.pone.0004212.g007

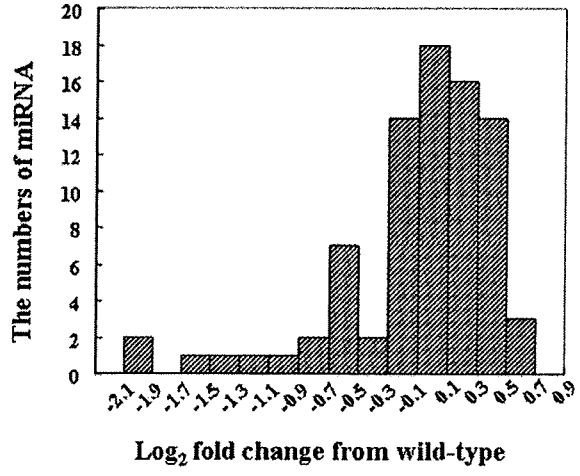

Figure 8. The distribution of changes in miRNA levels in *Dicer1*-hypomorphic mice compared to wild-type mice.
doi:10.1371/journal.pone.0004212.g008

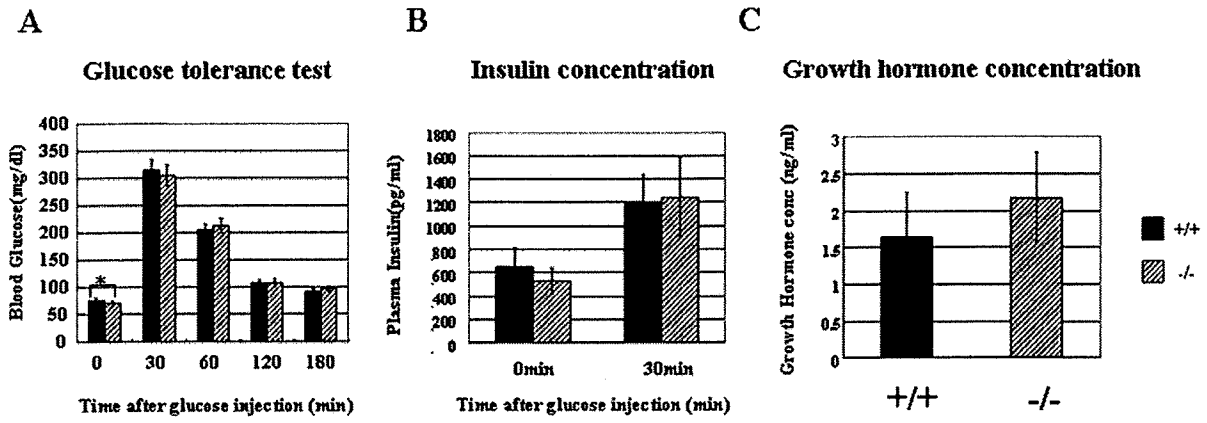

Figure 9. Glucose metabolism and growth hormone levels in wild-type and *Dicer1*-hypomorphic mice. A: Glucose tolerance test. Fasted 8-week-old mice received an intraperitoneal injection of glucose (2 mg/g body weight). B: Insulin concentration. Plasma insulin was measured before and after the intraperitoneal glucose injection. C: Growth hormone concentration. Plasma growth hormone concentrations were measured in wild-type and *Dicer1*-hypomorphic mice. A, B: Values are expressed as the means±S.D. (n = 20 per group). C: Values are expressed as the means±S.D. (n = 10 per group).*, $P<0.05$.
doi:10.1371/journal.pone.0004212.g009

C57BL/6 mice. *Dicer1* heterozygous mice were backcrossed with C57BL/6 mice for 12 generations. All animal experiments were approved by the Animal Research Ethics Board at the Gunma University.

Histochemistry and immunohistochemistry

Tissues and embryos were fixed overnight in formalin at 4°C and embedded in paraffin. Standard techniques were used for the embedding, sectioning and staining of tissues. Sections were cut at 5 μm. Immunohistochemistry was performed as follows: The slides were dewaxed and washed in PBS, and blocked in 1% BSA for 30 min. They were then incubated with primary antibodies overnight at 4°C in PBS containing 1% BSA, washed in PBS, and incubated with the appropriate secondary antibodies for 1 hour at room temperature. The slides were washed in PBS and mounted with Pristine Mount (Parma) with DAPI. The primary antibodies used were rabbit anti-glucagon (1:200, DAKO) and guinea pig anti-insulin (1:200, DAKO), rabbit Ki67 monoclonal antibody (Lab Vision), and Pdx1 (a gift from Christopher V. Wright (Vanderbilt University, Nashville)). The secondary antibodies were conjugated to rodamin (1:200, Jackson) and Alexa 488 (1:200, Molecular Probes). The slides were examined with a Nikon ECLIPSC TE300 and images were obtained with a LEICA DFC400 camera.

Measurement of islet area

ß-cell mass was measured using Image J software (NIH). Islet numbers and areas were averaged from 6 animals, with six sections from each animal, 250 μm apart.

RNA extraction and quantitative RT-PCR

Total RNA was prepared from isolated tissues using the RNeasy mini kit (Qiagen) with a modified protocol to purify total RNA containing miRNA from animal tissues. Differential gene expression was confirmed using the SYBR Premix Ex Taq (TAKARA) in accord with the manufacturer's instructions. The reaction was performed using the SYBER Green program on an ABI PRISM 7700 sequence detector system (Applied Biosystems). The expression of mRNA was normalized to that of GAPDH mRNA.

Primer sequences were as follows, ActRIIA: 5′-AGCGGAG-CTGACAGTGATTT-3′, 5′-CATACACGCACAACACACCA-3′ ActRIIB: 5′-TGGACATCCATGAGGTGAGA-3′, 5′-CAGCAG-CTGTAGTGGCTTCA-3′

miRNA microarray

Small RNAs were labeled with a miRNA labeling Reagent & Hybridization Kit (Agilent) based on the manufacturer's instructions. The Cy3-labeled RNA molecules were hybridized with a Mouse miRNA microarray (Agilent), consisting of control probes, mismatch probes, and 567 capture probes as registered and annotated in Sanger miRBase v10.1. A DNA MicroArray Scanner (Agilent) was used to scan images. The scanned images were analyzed with Agilent Feature Extractin Ver.9.5.3 (Agilent). Data were normalized globally per array. The net intensity values were normalized to per-chip median values.

Glucose tolerance test and insulin concentration

After overnight fasting, 2 mg/g (body weight) of glucose was administered intraperitoneally. Blood samples were drawn intraperitoneally from the tail at different times, and the blood glucose concentration was measured with an automatic blood glucose meter, Freestyle Freedom (NIPRO). Whole blood was collected and centrifuged, and the plasma was stored at −80°C. The insulin concentration was measured with an insulin measurement kit (Morinaga) in accordance with the manufacturer's instructions.

Growth hormone measurements

Growth hormone concentrations of wild-type and *Dicer1*-hypomorphic mice were measured with a rat/mouse growth hormone ELISA kit (LINCO Research).

Data analysis

Data were analyzed by the one-sample t-test and independent samples t-test. Data are the means±S.D.

Acknowledgments

We thank the Mutant Mouse Regional Resource Center (MMRRC) for providing RRF266 cells.

Author Contributions

Conceived and designed the experiments: SM IH. Performed the experiments: SM AH TH MK TK KN RM. Analyzed the data: SM IK TK TO KM. Contributed reagents/materials/analysis tools: SM. Wrote the paper: SM.

References

1. Gregory RI, Yan KP, Amuthan G, Chendrimada T, Doratotaij B, et al. (2004) The microprocessor complex mediates the genesis of microRNAs. Nature 432: 235–240.
2. Bernstein E, Caudy AA, Hammond SM, Hannon GJ (2001) Role for a bidentate ribonuclease in the initiation step of RNA interference. Nature 409: 363–366.
3. Hammond SM, Boettcher S, Caudy AA, Kobayashi R, Hannon GJ (2001) Argonaute2, a link between genetic and biochemical analyses of RNAi. Science 293: 1146–1150.
4. Lagos-Quintana M, Rauhut R, Yalcin A, Meyer J, Lendeckel W, Tuschl T (2002) Identification of microRNA from mouse. Current Biology 12: 735–739.
5. Wienholds E, Kloosterman WP, Misaka E, Alvarez-Saavedra E, Berezikov E, et al. (2005) MicroRNA expression in zebrafish embryonic development. Science 309: 310–311.
6. Bernstein E, Kim SY, Carmell MA, Murchison EP, Alcorn H, et al. (2003) Dicer is essential for mouse development. Nat Genet 35: 215–217.
7. Yang WY, Yang DD, Songqing N, Sandusky GE, Zhang Q, et al. (2005) Dicer is required for embryonic angiogenesis during mouse development. J Biol Chem 280: 9330–9335.
8. Harfe BD, McManus MT, Mansfield JH, Hornstein E, Tabin CJ (2005) The RNaseIII enzyme Dicer is required for morphogenesis but not patterning of the vertebrate limb. Proc Natl Acad Sci USA 102: 10898–10903.
9. Harris KS, Zhang Z, McManus MT, Harfe BD, Sun X (2006) Dicer function is essesntial for lung epithelium morphogenesis. Proc Natl Acad Sci USA 103: 2208–2213.
10. Andl T, Murchison EP, Liu F, Zhang Y, Yunta-Gonzalez M, et al. (2006) The miRNA-processing enzyme Dicer is essential for morphogenesis and maintenance of hair follicles. Current Biology 16: 1041–1046.
11. Lynn FC, Skewes-Cox BAP, Kosaka Y, McManus MT, Harfe BD, et al. (2007) MicroRNA expression is required for pancreatic islet cell genesis in the mouse. Diabetes 56: 2938–2945.
12. Cobb BS, Nesterova TB, Thompson E, Hertweck A, O'Connor E, et al. (2005) T cell lineage choice and differentiation in the absence of the RNase III enzyme Dicer. J Exp Med 20: 1367–1373.
13. Fukasawa M, Morita S, Kimura M, Horii T, Ochiya T, et al. (2006) Genomic imprinting in Dicer1-hypomorphic mice. Cytogenet Genome Res 113: 138–143.
14. Habener JF, Kemp DM, Thomas MK (2005) Minireview: Transcriptional regulation in pancreatic development. Endocrinology 146: 1025–1034.
15. Ackermann AM, Gannon M (2007) Molecular regulation of pancreatic β-cell mass development, maintenance, and expansion. J Mol Endo 38: 193–206.
16. Dor Y, Brown J, Martinez OI, Melton DA (2004) Adult pancreatic beta-cells are formed by self-duplication rather than stem-cell differentiation. Nature 429: 41–46.
17. Teta M, Rankin MM, Long SY, Stein GM, Kushner JA (2007) Growth and regeneration of adult β cells dose not involve specialized progenitors. Dev Cell 12: 817–829.
18. Bonner-Weir S, Baxter LA, Schuppin GT, Smith FE (1993) A second pathway for regenerating of adult exocrine and endocrine pancreas. A possible recapitulation of embryonic development. Diabetes 42: 1715–1720.
19. Bertelli E, Bendayan M (1997) Intermediate endocrine-acinar pancreatic cells in duct ligation conditions. Am J Physiol Cell Physiol 273: C1641–C1649.
20. Bonner-Weir S, Toschi E, Inada A, Reits P, Fonseca SY, et al. (2004) The pancreatic ductal epithelium serves as apotential pool of progenitor cells. Pediatric Diabetes 5: 16–22.
21. Xu X, D'Hoker J, Stange G, Bonne S, De Leu N, et al. (2008) β cells can be generated from endogenous progenitors in injured adult mouse pancreas. Cell 132: 197–207.
22. Kritzik MR, Jones E, Chen Z, Krakowski M, Krahl T, et al. (1999) Pdx-1 and Msx-2 expression in the regenerating and developing pancreas. J Endocrinol 163: 523–530.
23. Song SY, Gannon M, Wahington MK, Scoggins CR, Meszoely IM, et al. (1999) Pdx-1 expressing pancreatic epithelium and islet neogenesis in transgenic mice overexpressing transforming growth factor alpha. Gastroenterology 117: 1416–1426.
24. Shiozaki S, Tajima T, Zhang YQ, Furukawa M, Nakazato Y, et al. (1999) Impaired differentiation of endocrine cells of pancreas in transgenic mouse expressing the truncated type II activin receptor. Biochimica et Biophysica Acta 1450: 1–11.
25. Attisano L, Wrana JL, Cheifetz S, Massague J (1992) Novel activin receptors: dinsinct genes and alternative mRNA splicing generate a repertoire of serine/threonine kinase receptors. Cell 68: 97–108.
26. Mathews LS (1994) Activin receptors and cellular signaling by the receptor serine kinase family. Endocr Rev 15: 310–325.
27. Attisano L, Carcamo J, Ventura F, Weis FM, Massague J, et al. (1993) Identificatin of human activin and TGF beta type I receptors that form heteromeric kinase complexes with type II receptors. Cell 75: 671–680.
28. Yamashita H, Ten Dijke P, Huylebroeck D, Sampath TK, Andries M, et al. (1995) Osteogenic protein-1 binds to activin type II receptors and induce certain activin-like effectors. J Cell Biol 130: 217–226.
29. Lee SJ, McPherron AC (2001) Regulation of myostain activity and muscle growth. Proc Natl Acad Sci USA 98: 9306–9311.
30. Yeo C, Whitman M (2001) Nodal signals to Smads through Cripto-dependent and Cripto-independent mechanisms. Mol Cell 7: 949–957.
31. Oh SP, Yeo CY, Lee Y, Schrewe H, Whitman M, et al. (2002) Activin type IIA and type IIB receptors mediate Gdf11 signaling in axial vertebral patterning. Gene Dev 16: 2749–2754.
32. Gittes GK, Rutter WJ (1992) Onset of cell-specific gene expression in the developing mouse pancreas. Proc Natl Acad Sci USA 89: 1128–1132.
33. Teitelman G, Alpert S, Polak JM, Martinez A, Hanahan D (1993) Precursor cells of mouse endocrine pancreas coexpress insulin, glucagon and the neuronal proteins tyrosine hydroxylase and neuropeptide Y, but not pancreatic polypeptide. Development 118: 1031–1039.
34. Stryke D, Kawamoto M, Huang CC, Johns SJ, King LA (2003) BayGenomics: a resorce of insertional mutations in mouse embryonic stem cells. Nucleic Acids Res 31: 278–281.

Defined factors induce reprogramming of gastrointestinal cancer cells

Norikatsu Miyoshi[a], Hideshi Ishii[a,b,1], Ken-ichi Nagai[a], Hiromitsu Hoshino[a], Koshi Mimori[b], Fumiaki Tanaka[b], Hiroaki Nagano[a], Mitsugu Sekimoto[a], Yuichiro Doki[a], and Masaki Mori[a,b,1]

[a]Department of Gastroenterological Surgery, Osaka University Graduate School of Medicine, Osaka 565-0871, Japan; and [b]Department of Molecular and Cellular Biology, Division of Molecular and Surgical Oncology, Medical Institute of Bioregulation, Kyushu University, Ohita 874-0838, Japan

Communicated by Takashi Sugimura, National Cancer Center, Tokyo, Japan, November 4, 2009 (received for review August 11, 2009)

Although cancer is a disease with genetic and epigenetic origins, the possible effects of reprogramming by defined factors remain to be fully understood. We studied the effects of the induction or inhibition of cancer-related genes and immature status-related genes whose alterations have been reported in gastrointestinal cancer cells. Retroviral-mediated introduction of induced pluripotent stem (iPS) cell genes was necessary for inducing the expression of immature status-related proteins, including Nanog, Ssea4, Tra-1-60, and Tra-1-80 in esophageal, stomach, colorectal, liver, pancreatic, and cholangiocellular cancer cells. Induced cells, but not parental cells, possessed the potential to express morphological patterns of ectoderm, mesoderm, and endoderm, which was supported by epigenetic studies, indicating methylation of DNA strands and the histone H3 protein at lysine 4 in promoter regions of pluripotency-associated genes such as *NANOG*. In in vitro analysis induced cells showed slow proliferation and were sensitized to differentiation-inducing treatment, and in vivo tumorigenesis was reduced in NOD/SCID mice. This study demonstrated that pluripotency was manifested in induced cells, and that the induced pluripotent cancer (iPC) cells were distinct from natural cancer cells with regard to their sensitivity to differentiation-inducing treatment. Retroviral-mediated introduction of iPC cells confers higher sensitivity to chemotherapeutic agents and differentiation-inducing treatment.

cancer stem cells | epigenetics | pluripotent stem cells | embryonic stem cells | differentiation

Cancer is thought to be a genetic and epigenetic disease with uncontrolled proliferative potential. Although the idea was proposed decades ago, the concept that some cancer cells arise from small populations, termed cancer stem cells (CSCs), with both self-renewal potential and multipotential properties sufficient to form tumors, has emerged recently (1, 2). This small population of CSCs possesses persistent self-renewal potential that can be detected by various in vitro assessments and in vivo animal experiments (2). Therefore, it has been proposed that malignant tumors are derived from CSCs with uncontrolled proliferative potential and dysregulation of their mechanisms of differentiation (2).

The origins of CSCs remain incompletely understood (1–3). One view is that CSCs are formed as a result of alterations arising in cells that have already differentiated (1); alternatively, another notion holds that their generation is a result of tumorigenesis that has occurred in immature tissue stem cells or progenitor cells (2); however, in both theories, epigenetic organization participates in tumorigenic regulation (1, 2).

With the investigation and development of ES cells from zygote to blastodermic vesicle stages, the elucidation of the molecular mechanisms that specify pluripotent differentiation has made remarkable progress (4, 5). Regarding the regulation of molecular mechanisms managing this pluripotency, it is obvious that several types of transcription factors specifically discovered in multipotential stem cells display mutual cooperation as a result of epigenetic controls (6–9).

In this study, we analyzed the effects of transcription factor genes that were previously reported in induced pluripotent stem (iPS) cells (6, 7), as well as cancer-related oncogenes and tumor suppressor genes. The repression of tumor-suppressor genes extends the lifespan of embryonic stem (ES) cells or increases the induction efficiency of iPS cells and maintains their immortalized state (10–12). The results indicated that introduction of transcription factor genes into gastrointestinal cancer cells resulted in reprogramming of cells to a pluripotent state and sensitized them to differentiation induction. Such reprogrammed cells were distinct from parental cells. It is hoped that the generation of induced pluripotent cancer (iPC) cells will eventually accomplish some goals in this field. One such goal is the inspection of previously uncharacterized cancer treatments using differentiation therapy via the induction of drug susceptibility in cancer cells. Reprogramming of cancer cells supports the notion that transduction might cause differentiation of cells to unique cell lineages. Another goal is the exploitation of drug discoveries with the aim of producing therapeutic and diagnostic reagents and using them in their clinical applications.

Results

Expression of Genes Inducing Immature Status in Gastrointestinal Cancer Cell Lines. We performed quantitative real-time reverse transcription PCR (RT-PCR) analysis on 20 gastrointestinal cancer cell lines by using immature status-related gene primers for *NANOG, OCT3/4, SOX2, KLF4,* and *LIN28* (Fig. S1*A*). From the results of RT-PCR analysis, we selected cancer cell lines such as DLD-1, HCT116, MIAPaCa-2, and PLC, which exhibited relatively low *NANOG* mRNA expression. In these cells, immature status seems to be effectively exhibited and represented as high *NANOG* expression (6–9). Especially in the colorectal cancer cell line DLD-1, all five selected genes showed relatively low expression compared to the other gastrointestinal cancer cell lines. We then studied the induction of simultaneous combinations of several factors, which include *OCT3/4, SOX2, KLF4,* and *c-MYC,* as well as oncogenes (*BCL2* and *KRAS*) and tumor suppressor genes shRNA (*TP53, P16(INK4A), PTEN, FHIT, RB1*) (Fig. S1 *B* and *C*). These factors were transfected into four cancer cell lines with ecotropic retrovirus produced in PLAT-E packaging cells. Four transcription factors *OCT3/4, SOX2, KLF4,* and *c-MYC* significantly induced up-regulation of *NANOG* mRNA.

Induction of ES-Like State Cancer Cells with Lentiviral and Retroviral Transduction. Induction of human cancer cell lines using lentiviruses and retroviruses requires high transduction efficiencies. We optimized the transduction methods for cancer cell lines (Fig. 1*A*). The four transcription factors, *OCT3/4, SOX2, KLF4,* and *c-MYC,* were transfected into cancer cell lines with ecotropic retrovirus

Author contributions: N.M., H.I., and M.M. designed research; N.M. performed research; N.M. and H.I. contributed new reagents/analytic tools; N.M., H.I., K.N., H.H., K.M., F.T., H.N., M.S., Y.D., and M.M. analyzed data; and N.M. wrote the paper.

The authors declare no conflict of interest.

[1]To whom correspondence may be addressed. E-mail: hishii@gesurg.med.osaka-u.ac.jp or mmori@gesurg.med.osaka-u.ac.jp.

This article contains supporting information online at www.pnas.org/cgi/content/full/0912407107/DCSupplemental.

www.pnas.org/cgi/doi/10.1073/pnas.0912407107

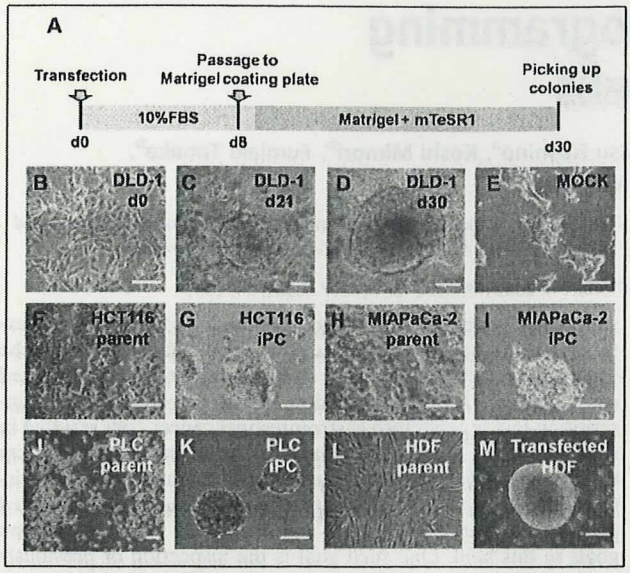

Fig. 1. Induction of human cancer cells with retroviral transduction. (*A*) We optimized the time course of the induction from human cancer cells; the schedule is summarized. (*B–E*) DLD-1 morphology was exhibited. Twenty days later, we observed distinct types of colonies with round shapes (*C* and *D*) that were different from the wild type (*B*). (*E*) Mock was transfected with pMXs Retroviral Vector as a negative control . (*F–K*) Parental and iPC cells of gastrointestinal cancer cell lines from HCT116 (*F* and *G*), MIAPaCa-2 (*H* and *I*), and PLC (*J* and *K*). (*L* and *M*) The referential morphologies are exhibited by HDF. Scale bar: 200 μm. (Original magnification, ×200)

produced in PLAT-E packaging cells. Eight days after transduction, the cells were harvested by trypsinization and plated onto Matrigel-coated plates. The next day, the Dulbecco's modified Eagle medium (DMEM) containing 10% FBS was replaced with the medium suitable for the culture of ES cells. Twenty-one days later, some colonies appeared that were morphologically different from the parental cancer cells (Fig. 1 *B* and *C*). Four weeks after transduction, we observed distinct types of colonies that were different from mock cells, transfected with pMXs retroviral vector as negative control (Fig. 1 *D* and *E*).

We examined the transfection and induction efficiencies by using combinations of *OCT3/4*, *SOX2*, *KLF4*, and *c-MYC*, and compared the results, with four cancer cell lines and human dermal fibroblasts (HDF) serving as controls (Fig. 1 *F–M*). In isolated colonies, we assessed *NANOG* promoter activity, which has been reported to be important in the acquisition of immature status (6–9), by co-transfection of *NANOG* promoter-*GFP* clone. *GFP* expression of transfectants was visualized by fluorescence microscopy (Fig. S2). From 1×10^4 cancer cells, we observed ≈10 *GFP*-expressing sphere formations. These cells in the present study were similar to iPS cells both in morphology, ES-like gene expression and epigenetic modifications as described in refs. 6–9, 13, and 14. Thus, we referred to these cells formed after transduction as iPC cells.

iPC Cells Express ES Cell Markers. Real-time RT-PCR using primers specific for retroviral transcripts confirmed efficient silencing of four retroviruses expressing *OCT3/4*, *SOX2*, *KLF4*, and *c-MYC* in iPC cells (Fig. 2*A*). RT-PCR showed that human iPC cells expressed undifferentiated ES cell-marker genes, including *NANOG*, *OCT3/4*, *SOX2*, *KLF4*, and *c-MYC*, although *NANOG* was not introduced exogenously (Fig. 2*B*). iPC cells expressed ES cell-specific surface antigens (15) including Ssea-4, tumor-related antigen (Tra)-1-60, Tra-1-81, and Tra-2-49 (Fig. 2 *C–G*) compared to the negative control (Fig. 2*H*).

In Vitro Differentiation of iPC Cells. To determine the differentiation ability of iPC cells, we used floating cultivation as embryoid bodies (EBs). Because iPC cells formed ball-shaped structures in suspension culture, we transferred these EB-like structures to EB culture conditions (EBC). These conditions were gelatin-coated plates maintained in DMEM/F12 containing 20% knockout-certified serum replacement. Culture was continued for another 7 days (Fig. 3*A*). Attached cells, named PostiPC cells, began to proliferate after 48 h. PostiPC cells were analyzed by the experiments described below and were compared to parental and iPC cells.

To determine the differentiation ability of iPC cells in vitro, we introduced iPC cells according to the methods of iPS (7). PostiPC cells showed various types of morphology, resembling those of epithelial cells, mesenchymal cells, and neuronal cells (Fig. 3 *B–E*). Immunocytochemistry detected cells that were positive for keratin 19 (Krt19) representing endoderm, vimentin (Vim) representing mesoderm and parietal endoderm, bIII-tubulin (Tubb3) representing ectoderm, and glial fibrillary acidic protein (Gfap) representing ectoderm (Fig. 3 *F–I*). RT-PCR confirmed, in addition to *VIM*, the expression of *FABP4* representing mesoderm, microtubule-associated protein 2 (*MAP2*) representing ectoderm, and paired box 6 (*PAX6*) representing ectoderm in PostiPC cells (Fig. 3*J*). The expression of *CDH1* representing endoderm and *KRT19* decreased in PostiPC cells. In particular, the gene expression of mesoderm and endoderm was increased in PostiPC cells, which was low or difficult to detect in the parental cells.

We then examined whether lineage-directed differentiation of iPC cells could be induced by methods reported for mesenchymal stem cells. We seeded iPC cells with supplements

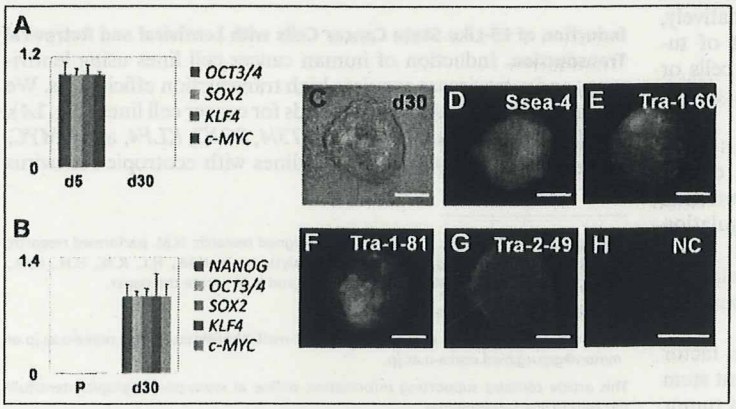

Fig. 2. iPC cells induced from DLD-1 expressing ES cell markers. (*A*) Real-time RT-PCR using primers specific for retroviral transcripts confirmed efficient silencing of four retroviruses expressing *OCT3/4*, *SOX2*, *KLF4*, and *c-MYC*. The mean value of d5 was set to 1 in each transcript. (*B*) iPC cells expressed undifferentiated ES cell-marker genes, including *NANOG*, *OCT3/4*, *SOX2*, *KLF4*, and *c-MYC*. The mean value of d30 was set to 1 in each transcript. (*C–G*) iPC cells were analyzed for several surface antigens, phase contrast (*C*), Ssea-4 (*D*), Tra-1-60 (*E*), Tra-1-81 (*F*), Tra-2-49 (*G*) and negative control (H). P, parental cells; NC, negative control. Scale bar: 200 μm. (Original magnification, ×200)

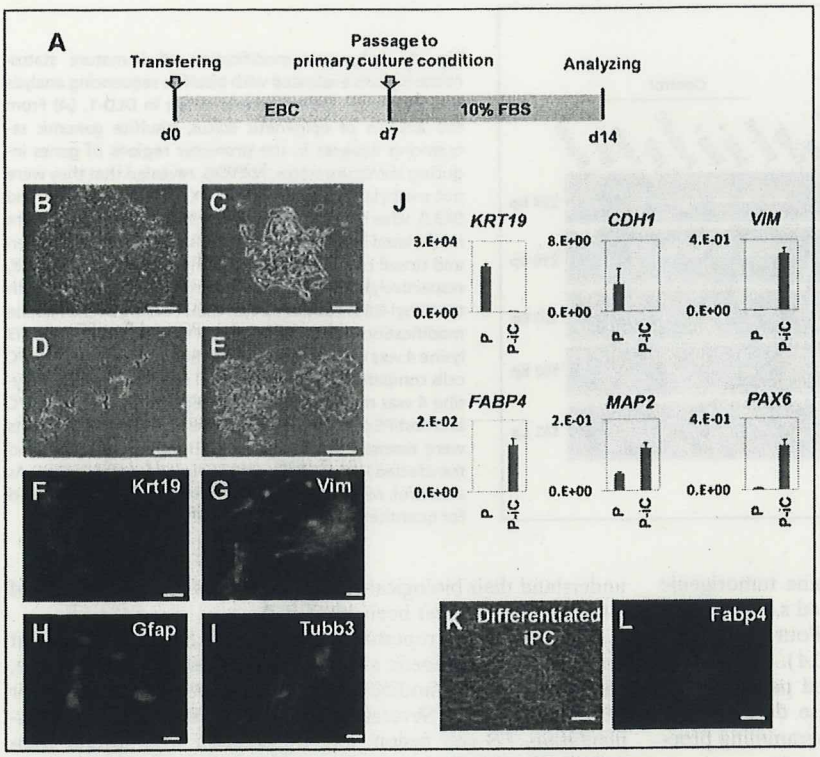

Fig. 3. Embryoid body (EB)-like formation mediated differentiation of iPC cells induced from DLD-1. (*A*) Schedule of induction from iPC cells to PostiPC cells. (*B–E*) After forming EB-like structures, iPC cells were transferred to primary culture conditions. Seven days later, attached (PostiPC) cells showed various morphologies, resembling those of epithelial cells (*B*), mesenchymal cells (*C*), neuronal cells (*D*), and mixed (*E*). (*F–I*) Immunocytochemistry confirmed the expression of Krt19 (*F*), Vim (*G*), Gfap (*H*), and Tubb3 (*I*) in these cells. (*J*) Real-time RT-PCR analysis verified the expression of differentiation markers, such as *KRT19, CDH1, VIM, FABP4, MAP2,* and *PAX6.* The expression of mRNA copies was normalized against *GAPDH* mRNA expression. (*K* and *L*) Directed differentiation of iPC cells into adipocytes showed differentiated iPC cells (*K*) that were positive for Fabp4 (*L*). P, parental cells; P-iC, PostiPC cells.

inducing adipocytes and maintained them under differentiation conditions for 2 weeks. The cells proliferated and immunocytochemistry detected cells positive for Fabp4 (Fig. 3 *K* and *L*). In contrast, immunocytochemistry on parental cells in the corresponding culture detected cells that were negative for Fabp4. These data demonstrated the possibility that iPC cells, compared to parental cells, could differentiate into three germ layers in vitro and indicated that cells acquired different properties.

Epigenetic Modification of Immature Status-Related Genes. Bisulfite genomic sequencing analyses were used to evaluate the methylation statuses of cytosine guanine dinucleotides (CpG) in the promoter regions of pluripotent-associated genes such as *NANOG*. The results revealed that the CpG dinucleotides of *NANOG* promoter were less methylated in transfected HDF (T-HDF) cells and two iPC clones, whereas the nucleotides were methylated in HDF, parental cancer cells, and PostiPC cells (Fig. 4*A*). Chromatin immunoprecipitation with trimethyl-histone H3 protein at lysine 4 (H3K4) antibody was used to analyze histone modification (Fig. 4*B*). The histone modification analyses for *NANOG* gene promoter showed that H3K4 was trimethylated in iPC, PostiPC, and T-HDF (14), whereas that of parental cancer cells and HDF was not detected. Similarly, the H3K4 trimethylation of *OCT3/4* gene promoter increased in iPC, PostiPC, and T-HDF, compared to parental cancer cells and HDF, respectively. The trimethylation of *SOX2* gene promoter was detected before and after the reprogramming of cancer cells, whereas the trimethylation of T-HDF, but not HDF, was detected. The trimethylation of *PAX6* and *MSX2* gene promoter was not detected. These findings demonstrated activation of the promoter regions of immature status-related genes in iPC cells.

Gene Expression and iPC and PostiPC Surface Markers. PostiPC cells, but not iPC cells, showed increased expression of several differentiation markers such as *FABP4, MAP2,* and *PAX6* (Fig. 3*J*), and markedly decreased expression of *NANOG*, *REX1*, *OCT3/4*, *SOX2*, *KLF4,* and *c-MYC*, which corresponded to those of parental cells (Fig. 5*A*). The expression of *P16(INK4A)* in PostiPC cells increased more than that in parental cells.

In colorectal cancer, the surface markers for CD24 and CD44 have been reported as CSC markers (16, 17). Flow cytometry showed that CD44 expression was markedly reduced in iPC cells and was increased in PostiPC cells. The CD44 expression level was relatively low in PostiPC cells compared with that of parental cells (Fig. 5*B*). CD 24 expression level was not changed apparently. The results showed the transition of the population from parental cells to PostiPC, suggesting an alteration of biological characteristics, such as sensitivity to chemicals.

Sensitivity of Anticancer Drug and Differentiation-Inducing Chemicals. The methyl thiazolyl tetrazolium (MTT) assay showed that PostiPC cells acquired sensitivity to 5-fluorodeoxyuridine (5-FU) to a greater degree than parental cells ($n = 11$, $P = 0.003$, Wilcoxon rank test; Fig. 6*A*). These data suggest the possibility that PostiPC cells, via iPC cells, could be more sensitive to therapeutic agents.

Proliferation assays for 48 h in Matrigel and the mTeSR1 medium, an ES-culture condition, showed that iPC cell growth significantly decreased compared with parental cells based on mean cell counts in four independent wells ($n = 4$, $P = 0.046$, Wilcoxon rank test; Fig. 6*B*). There was, however, no significant difference in 48-h proliferation of parental and PostiPC cells in primary culture conditions (Fig. 6*C*). An invasion assay showed no significant differences between parental and PostiPC cells (Fig. 6*D*). In a sharp contrast, the 48-h proliferation assays with the presence of retinoic acid (RA) and 1,25-dihydroxy vitamin D3 (VD3), which are known as inducers of differentiation (18, 19), resulted in a reduction in PostiPC cells compared with mock-treated parental cells ($n = 8$, $P = 0.512$ and 0.049, respectively, Wilcoxon rank test; Fig. 6 *E* and *F*). Invasion assays were performed after the 48-h treatment; the data indicated that, in the presence of RA and VD3, the invasion activity of PostiPC cells was reduced compared with parental cells ($n = 6$, $P = 0.013$ and 0.003, respectively, Wilcoxon rank test; Fig. 6 *G* and *H*).